

JGR Biogeosciences

RESEARCH ARTICLE

10.1029/2019JG005149

Key Points:

- We measured leaf wax hydrogen (δD_{wax}) and carbon ($\delta^{13}C_{wax}$) isotopes in plants and soils across a climate transect in Israel
- In areas containing only C_3 plants (rainfall 500 to 1,300 mm/year), soil $\delta^{13}C_{wax}$ is constant
- Soil δD_{wax} correlates with rainfall isotopic composition, and the rainfall to leaf wax isotopic offset correlates with relative humidity

Supporting Information:

- Supporting Information S1
- Table S1

Correspondence to:

Y. Goldsmith,
yonig@mail.huji.ac.il

Citation:

Goldsmith, Y., Polissar, P. J., deMenocal, P. B., & Broecker, W. S. (2019). Leaf wax δD and $\delta^{13}C$ in soils record hydrological and environmental information across a climatic gradient in Israel. *Journal of Geophysical Research: Biogeosciences*, 124, 2898–2916. <https://doi.org/10.1029/2019JG005149>





Received 18 MAR 2019

Accepted 6 JUN 2019

Accepted article online 16 AUG 2019

Published online 11 SEP 2019

Leaf Wax δD and $\delta^{13}C$ in Soils Record Hydrological and Environmental Information Across a Climatic Gradient in Israel

Yonaton Goldsmith^{1,2} , Pratigya J. Polissar¹ , Peter B. deMenocal¹ , and Wallace S. Broecker^{1,3} 

¹Lamont-Doherty Earth Observatory, Columbia University, Palisades, NY, USA, ²Now at Institute of Earth Sciences, Hebrew University of Jerusalem, Jerusalem, Israel, ³Deceased, currently drawing down CO₂ at the bottom of the Southern Ocean

Abstract The hydrogen (δD_{wax}) and carbon ($\delta^{13}C_{wax}$) isotope compositions of long-chain alkanes derived from plant waxes record hydrological and environmental conditions. However, the integration of plant n -alkanes into the sedimentary cycle, the variability of δD_{wax} and $\delta^{13}C_{wax}$ in soils, and the paleoclimate applicability in paleosols and archaeological sediments are poorly constrained. We sampled plants and soils across a steep climate transect in Israel to understand how plant type and environmental parameters shape $\delta^{13}C_{wax}$ and δD_{wax} . This transect has three advantages: existence of long-term precipitation isotopic composition (δD_r) records, a single wet season potentially reduces variability due to seasonality, and abandoned Byzantine period (~300–600 AD) agricultural terraces that reduce modern and ancient soil mixing and provide age constraints. We find that soil $\delta^{13}C_{wax}$ is constant (0.4‰, 1σ) across a 500- to 1,300-mm/year rainfall gradient and appears insensitive to rainfall amount, unlike bulk plant $\delta^{13}C$. The absence of a rainfall effect suggests that $\delta^{13}C_{wax}$ may be better suited to reconstructing C_3/C_4 plant ratios than bulk $\delta^{13}C$. Homologue average soil δD_{wax} significantly correlate with δD_r , and the offset between δD_r and soil δD_{wax} (ϵ_{app}) correlates with growing season relative humidity. The seasonality of leaf production accounted for at most ~10% of total plant δD_{wax} variability. Lastly, soil δD_{wax} and $\delta^{13}C_{wax}$ variability is reduced by ~80% relative to plant δD_{wax} and $\delta^{13}C_{wax}$ variability. Our results show that soil δD_{wax} and $\delta^{13}C_{wax}$ faithfully record δD_r and landscape C_3 - C_4 plant contributions and thus support the utility of these proxy data in paleosols and archaeological sites.

Plain Language Summary The influence of climate on biological and social human evolution has been an important research topic in recent decades. Isotopic analysis of leaf wax molecules from soil horizons and sediments from paleontological and archaeological sites can potentially offer climatic and environmental context directly associated with the sites. We conducted a calibration test across a climate transect in Israel to understand how plant type and environmental parameters impact the isotopic composition of leaf wax molecules in soils. Our results show that leaf wax carbon isotopes in soils are constant in the range of 500 to 1,300 mm/year and thus are suitable for reconstructing the contribution of C_3 and C_4 plants to the soils. The leaf wax hydrogen isotopes in soils are correlated with the isotopic composition of rainfall and the relative humidity of the growing season. Our results support the utility of these proxy data in paleosols and archaeological sites.

1. Introduction

The influence of climate on biological and social human evolution has been an important research topic in recent decades. Efforts have often focused on reconstructing the local climatic and environmental contexts of central locations of human evolution (d'Alpoim Guedes et al., 2016; deMenocal, 2011; National Research Council, 2010; e.g., Potts, 1996; Quade, 2014). Isotopic analysis of leaf wax molecules from soil horizons (paleosols) and sediments from paleontological, paleoanthropological, and archaeological sites can potentially offer climatic and landscape context directly associated with the archaeological record (e.g., Magill et al., 2013; Uno et al., 2016). Leaf wax analysis can add to the existing environmental proxies (e.g., $\delta^{13}C$ and clumped isotopes in soil carbonates; Levin, 2015; e.g., Quade, 2014), pollen and phytoliths (for recent compilation see Bonnefille, 2010) and lignin (Magill et al., 2016), and assist in understanding the possible links between the environment and biological and cultural evolution.

Carbon ($\delta^{13}\text{C}_{\text{wax}}$) and hydrogen ($\delta\text{D}_{\text{wax}}$) isotopic compositions of long-chain normal alkane (henceforth *n*-alkane) compounds in leaf waxes of terrestrial plants reflect the growth environment and phylogeny of the plants (e.g., Diefendorf et al., 2011; Sachse et al., 2012). However, individual plants show considerable $\delta^{13}\text{C}_{\text{wax}}$ and $\delta\text{D}_{\text{wax}}$ variability even within species or plant functional type, and thus, plant $\delta^{13}\text{C}_{\text{wax}}$ and $\delta\text{D}_{\text{wax}}$ distributions contain significant variability uncorrelated with environmental parameters (e.g., Sachse et al., 2012). The *n*-alkanes are durable molecules; they withstand weathering and to some extent bacterial degradation (e.g., Chikaraishi & Naraoka, 2006; Nguyen Tu et al., 2011; Pond et al., 2002; Tuthorn et al., 2015; Zech et al., 2011), and are incorporated into the sedimentary cycle and accumulate in soils and lakes (e.g., Lichtfouse et al., 1998; Pedentchouk et al., 2006). Throughout this process, leaf waxes are integrated over space and time, and soil $\delta^{13}\text{C}_{\text{wax}}$ and $\delta\text{D}_{\text{wax}}$ variability is reduced. By the time leaf wax *n*-alkanes are deposited in lakes, the $\delta\text{D}_{\text{wax}}$ and $\delta^{13}\text{C}_{\text{wax}}$ variability is reduced at least threefold in respect to that of plant tissues, to an extent that $\delta\text{D}_{\text{wax}}$ shows a significant correlation with rainfall δD and can be applied to study past climate (Garcin et al., 2012; Guenther et al., 2013; Hou et al., 2008; Polissar & Freeman, 2010; Sachse et al., 2004). However, it is less clear where in the sedimentary cycle the homogenization process and variability reduction occurs, what processes are involved (Feakins et al., 2018; Huang et al., 1997; Mazeas et al., 2002; Mendez-Millan et al., 2014; Nguyen Tu et al., 2011; Zech et al., 2011) and how well soil $\delta^{13}\text{C}_{\text{wax}}$ and $\delta\text{D}_{\text{wax}}$ reflect the parent plant material (Chikaraishi & Naraoka, 2006; Garcin et al., 2014). Specifically, we are interested in understanding where the homogenization process occurs and to what extent the variability at the leaf and plant level is reduced in soils. Does it occur in the initial phase of soil formation or does the integration require a larger spatial averaging that can only occur at lake basin scales? This distinction is important: If a significant portion of the $\delta\text{D}_{\text{wax}}$ and $\delta^{13}\text{C}_{\text{wax}}$ homogenization occurs in the early phases of soil formation, then it would be possible to use soil $\delta\text{D}_{\text{wax}}$ and $\delta^{13}\text{C}_{\text{wax}}$ to reconstruct environmental and climatic signals from paleosols and archaeological sites.

Here we analyze leaf wax $\delta^{13}\text{C}_{\text{wax}}$ and $\delta\text{D}_{\text{wax}}$ and chain length distributions across a strong climate and vegetation gradient to understand how environmental factors shape the leaf wax signal at the plant level, how this signal is recorded in soils, and the uncertainty of this signal when applied to reconstruct environmental conditions from paleosols. We conducted a field-based test along a climate transect in Israel where rainfall ranges from 70 to 1,300 mm/year and growing season relative humidity from 60% to 80%. The large climate gradient, a single well-defined rainy season, long-term monitoring of water isotopes in rainfall, and ancient agricultural terraces with defined ages make this region highly suitable to assess the controls and variability of leaf wax $\delta\text{D}_{\text{wax}}$ and $\delta^{13}\text{C}_{\text{wax}}$ in soils. This study contributes to the understanding of how the integration of leaf wax molecules into soils shapes their relationship to environmental variables and the robustness of using $\delta\text{D}_{\text{wax}}$ and $\delta^{13}\text{C}_{\text{wax}}$ in soils as climatic and environmental proxies. Quantifying the uncertainty of these proxies will also improve the use of paleosols and sediments from archaeological sites to reconstruct environmental conditions.

2. Background

2.1. Factors Affecting $\delta^{13}\text{C}_{\text{wax}}$

In plants using the C_3 photosynthetic pathway, bulk leaf carbon isotopes ($\delta^{13}\text{C}_{\text{bulk}}$) vary as a function of CO_2 concentration (e.g., Farquhar et al., 1982; Schubert & Jahren, 2012), annual rainfall (e.g., Diefendorf et al., 2010; Kohn, 2010), and light levels (e.g., Graham et al., 2014). Plants using the C_4 pathway have more positive carbon isotope values and are largely insensitive to the environmental parameters driving variability in C_3 plants (e.g., Farquhar et al., 1982; O'Leary, 1981). Leaf wax $\delta^{13}\text{C}_{\text{wax}}$ is offset from bulk plant tissues ($\delta^{13}\text{C}_{\text{bulk}}$) by about -8‰ (C_4) to -3‰ (C_3 ; Collister et al., 1994; Diefendorf & Freimuth, 2017; Tipple & Pagani, 2010). This offset, ϵ_{lipid} , differs as a function of plant type (Chikaraishi & Naraoka, 2006), and variations of up to 10‰ have been shown (Diefendorf et al., 2011). Previous research indicates that $\delta^{13}\text{C}_{\text{wax}}$ of C_3 plants is moderately correlated with annual rainfall and relative humidity (Garcin et al., 2014) and altitude (Feakins et al., 2018; Wu et al., 2017). $\delta^{13}\text{C}_{\text{wax}}$ of C_4 plants in a transect in Cameroon show no correlation with rainfall or humidity (Garcin et al., 2014). Soil $\delta^{13}\text{C}_{\text{wax}}$ from the Cameroon transect shows a weak significant correlation with relative humidity (Schwab et al., 2015), and those from a transect in China show an altitude effect similar to that in bulk $\delta^{13}\text{C}$ (Wei & Jia, 2009). Whether these findings are applicable to regions beyond those studied is something we investigate here.

2.2. Factors Affecting δD_{wax}

Across global data sets, rainfall δD (δD_r) is the strongest predictor of δD_{wax} (Aichner et al., 2010; Polissar & Freeman, 2010; Sachse et al., 2004, 2006, 2012; Smith & Freeman, 2006). However, at the local scale, plant type, leaf transpiration, and soil evaporation can modify the δD_{wax} signal (Kahmen et al., 2013; Sachse et al., 2012; Tipple et al., 2014). Different plant types exhibit distinct offsets from rainfall δD and are an important factor to consider when interpreting fossil δD values. Evaporation of source water prior to uptake by plants can result in more positive δD_{wax} values, and leaf-level transpiration driven by water vapor pressure deficit enriches leaf water δD and δD_{wax} . The observed natural variability of the offset between δD_{wax} and δD_r in plants is $>50\%$ (Sachse et al., 2012). At the plant-functional-type level, variability decreases to $\sim 30\%$ and drops further to 10–30% in lake sediments (Garcin et al., 2012; Hou et al., 2007; Polissar & Freeman, 2010). Here we evaluate how plant-level variability is related to the integrated signal in soils across a large gradient in rainfall amount and vegetation type.

2.3. Chain Length Distribution Variability

The distribution of plant-wax *n*-alkanes have been proposed to respond to environmental parameters (Bush & McInerney, 2015; Howard et al., 2018; Sachse et al., 2006; Schefuß et al., 2003; Vogts et al., 2012) and plant type (e.g., Bush & McInerney, 2013; Garcin et al., 2014; Rommerskirchen et al., 2006; Vogts et al., 2012). Though a large compilation of observations has not found such relations at a global scale (Bush & McInerney, 2013), at the continental scale, meaningful relationships may still be significant (e.g., Bush & McInerney, 2013; Vogts et al., 2012). Here we examine the utility of leaf wax distributions in paleoclimate reconstructions by measuring leaf wax distributions in plants and soils across a large climate gradient.

2.4. Possible Sources of Uncertainty in Plant Wax Calibration Data Sets

Three important factors likely affect leaf wax signals and may not be resolved in many existing calibration data sets: the seasonality of leaf wax production and rainfall, measurements of rainfall δD , and the time integrated in *modern* sediments.

2.4.1. Seasonality

The amplitude of the seasonal rainfall cycle and δD_r and timing of leaf production within the growing cycle of the plant have been proposed as important contributors to δD_{wax} , $\delta^{13}C_{wax}$, and chain length distribution variability (Berke et al., 2015; Collins et al., 2013; Freimuth et al., 2017; Schwab et al., 2015; Tipple et al., 2013). To address this issue, we chose a sampling location that has only one rainy season and a large majority of the plants produce their leaves during or directly after the rainy season.

2.4.2. Rainfall δD Values

The δD of rainfall is one of the essential parameters in calibration data sets. Previous research has used model data (Berke et al., 2015; Kahmen et al., 2013; Peterse et al., 2009; Sachse et al., 2006), limited rainfall sampling (e.g., Garcin et al., 2012; Schwab et al., 2015), river, soil, and groundwater observations (e.g., Jia et al., 2008; Sachse et al., 2006; Schwab et al., 2015), xylem water (e.g., Feakins & Sessions, 2010), and leaf water (Freimuth et al., 2017) as the source water for calculating δD_{wax} fractionation. Using model extrapolations as the basis for δD_r can be a source of error (e.g., Feakins & Sessions, 2010) that may increase the apparent variability of δD_{wax} fractionation. Limited temporal observations can result an inaccurate assessment of the δD_r mean value. To reduce these possible sources of uncertainties, here, sampling was conducted adjacent to rainfall monitoring stations that have been measuring the isotopic composition of rainfall for ~ 20 years and thus provide a well-constrained δD_r mean value (Figure 1).

2.4.3. Age of Modern Samples

Leaf wax calibration studies of sediments (soils, lake, and ocean sediments) assume a modern age for the calibration samples. However, it can often be difficult to quantify the time integrated in a modern sediment sample because vertical mixing and accumulation rates are not always known. In soils, sampling of unstable landforms or soils of unknown age may be a source of uncertainty due to mixing of soils of different ages. To reduce this possible source of variability, we sampled abandoned agricultural terraces built during the Byzantine period (~ 300 –600 AD). These terraces are wide and flat step-like structures that reduce soil movement and mixing and enable attribution of the upper 2-cm soil horizon as modern or submodern (<1.7 ka). We cannot rule out the possibility that old soils and/or windblown material have been mixed into the soils;

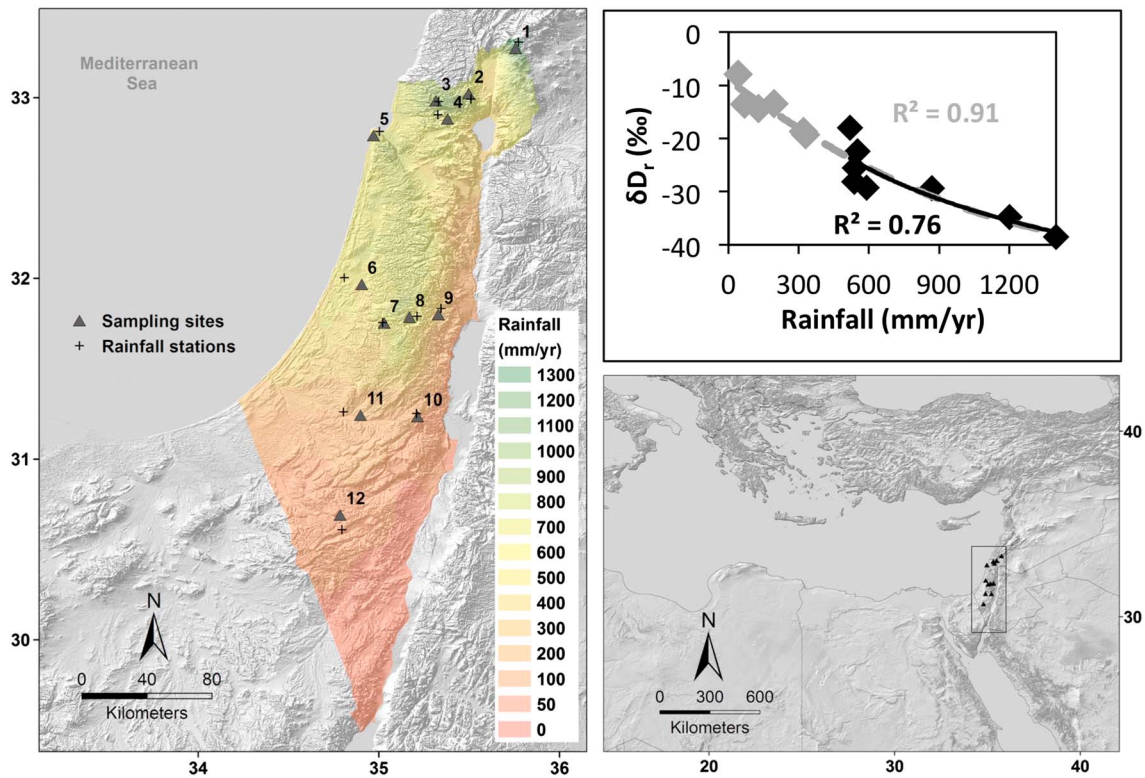


Figure 1. Annual rainfall map of the study area, with sampling sites (triangles) and rainfall stations (plus sign). Eastern Mediterranean and study sites (bottom right). Correlation between annual rainfall and the δD_r , black line and r^2 are only Mediterranean sites (from Goldsmith et al., 2017), and gray dashed line and r^2 are all sites (top right).

however, we argue that sampling abandoned terraces substantially reduces this mixing and thus is the closest natural test representing the local in situ leaf production and soil formation.

3. Study Area

3.1. Climate and Geography

The eastern Mediterranean has warm-dry summers and cold-wet winters. Rainfall occurs almost exclusively during October to April, with most rainfall falling between December and February (Ziv et al., 2006). The topography of Israel can be divided into three areas from west to east: the coastal plain, a north-south mountains region, and the Dead Sea Valley (Figure 1). Precipitation generally correlates with temperature and altitude, where higher precipitation falls at higher and colder elevations (Figure 1). In addition, temperature decreases and rainfall increases from south to north (Figure 1), where the southern part of Israel lies in the global desert belt and the northern part has a Mediterranean climate. The Dead Sea Valley is a local rain-shadow desert.

3.2. Vegetation

From a photosynthetic pathways perspective, ecosystems in Israel are divided into two main regions, a pure C₃ ecosystem in the Mediterranean region and a mixed C₃/C₄ (~75% C₃) ecosystem in the desert areas (Vogel et al., 1986; Winter & Troughton, 1978). The common C₄ plants in Israel are dicots and not monocot grasses as is common in other places in the world and thus pose an interesting question regarding their δD_{wax} and $\delta^{13}C_{wax}$ signals. Hartman and Danin (2010) measured bulk plant $\delta^{13}C$ along a similar transect to that presented in this paper, albeit at different sites. They conclude that bulk $\delta^{13}C$ of C₃ plants is significantly correlated with rainfall amount (though, $r^2 = 0.14$) and bulk $\delta^{13}C$ of C₄ plants are not correlated with rainfall amount. Similar findings have been reported elsewhere for C₃ (e.g., Diefendorf et al., 2010; Kohn, 2010,) and C₄ plants (e.g., Peisker & Henderson, 1992).

3.3. Isotopic Composition of Precipitation

The isotopic composition of rainwater in Israel has been monitored at 12 stations by A. Ayalon and M. Bar-Matthews from the Geological Survey of Israel over the past ~20 years (Ayalon et al., 2004; Goldsmith et al., 2017) and at two stations (Beit Dagan and Har Canaan) by J. Gat in the 1970s to 1980s. These monitoring stations span almost the entire length of Israel; they have a precipitation range of 40 to 1,300 mm/year (Figure 1) and an elevation range 0 to 1,400 m above sea level. The resolution (daily/monthly) and amount of years measured vary between sites (full details in Goldsmith et al., 2017). The long-term isotopic composition of precipitation in Israel is governed primarily by the isotopic composition of the Mediterranean sea surface, normalized humidity over the Mediterranean (i.e., relative humidity normalized to sea surface temperature), and sea surface to land temperature gradient that drives the distillation effect. The average isotopic composition of rainfall in Israel shows high correlations with rainfall amount ($r^2 = 0.9$ for δD ; Figure 1), altitude ($r^2 = 0.85$), and distance from the ocean ($r^2 = 0.58$; Goldsmith et al., 2017). The distances from the sea, elevation, temperature, and latitude are all correlated, all driving the isotopic composition in the same direction. In addition, the short transport distance (<100 km) prevents significant moisture recycling. δD_r in sites located in the desert region is affected by evaporation during the rain event, which does not affect sites located in the Mediterranean region. This high temporal and spatial resolution of δD_r together with a large rainfall gradient make it ideal for constraining the interpretation of δD_{wax} of different environments.

4. Methods

4.1. Sampling Methods

Using the archaeological literature, we located Roman-Byzantine sites within a radius of ~5 km from each modern rainfall monitoring station (see Appendix A in the supporting information for full site descriptions). Throughout the paper, we divide the sites into Mediterranean sites ($n = 8$) where rainfall is >400 mm/year and δ_r falls on the East Mediterranean meteoric water line (Goldsmith et al., 2017) and desert sites ($n = 4$) where rainfall is <400 mm/year and δ_r shows evaporative enrichment during rainfall events. Using air photos, we located agricultural terraces in an area of a few hundred meters around the archeological sites and assumed the terraces date to the time of the archaeological sites. At each site, we chose the least disturbed terrace (e.g., flat, not cut by gullies and supporting walls intact) and dug a soil pit into the sediments confined by the terrace wall (assuming that this is the most protected area). The pit was dug to the bedrock or to the top of the archaeological horizon. The soil section was logged and described according to standard U.S. soil description terminology and methods (Soil Survey Staff, 1999). Most of the profiles showed no real soil horizons, indicating that these are very young and immature soils. Therefore, rather than using the standard term *horizon*, the profiles were divided into *units* based on color or structure changes. The top 2–3 cm of each soil profile were sampled. Plant material was sampled from the most abundant plants within a radius of <10 m from the soil section. One to four leaf samples of different plants were collected at each site. For each tree or shrub sample, ~20 leaves from various parts of the same plant were collected. Grasses were collected whole from a few ($n = 5$ to 10) adjacent individual plants. Each sample was placed in aluminum foil, labeled, sealed, and placed in a marked zip-lock bag. In the lab, the plants were identified using the Flora of Israel Online (<http://flora.org.il/en/avinoam-danin-2/>, accessed October 2015) and flowering season was noted. Sampling was conducted in summer of 2013; during this season the annual plants were dry, and therefore, not all plants could be identified to the species level (Table S2-4).

4.2. Laboratory Procedures

The soils were lyophilized overnight (-70 °C at 50×10^{-3} mb). All roots and visible plant material were removed. Organic molecules were extracted from ~30 g of soils using a Dionex Accelerated Solvent Extractor 350 with 60-ml extraction cells. We used 9:1 dichloromethane:methanol (DCM:MeOH v/v) for the extraction and four 10-min static cycles at 100 °C with a flush volume of 150%. The number of cycles and hold time were needed to completely extract *n*-alkanes from the soils.

The plants were lyophilized overnight (-70 °C at 50×10^{-3} mb). The plants were dry, and the leaves appeared unblemished, so no additional cleaning was done. The organic molecules were extracted from ~0.5 g of dried leaves using hexane by ultrasonic agitation. Samples were sonicated three times for

20 min. After each round of sonication, the extract was removed and replaced with fresh hexane. The three extracts were combined to form the total lipid extract (TLE).

To trace possible sample loss throughout the procedure and to quantify *n*-alkane concentration, 2,000 ng of a laboratory standard (5 α -androstane) was added to each soil and plant TLE.

Solvent from the TLE extraction (Accelerated Solvent Extractor and sonication) was evaporated under a stream of N₂, and the TLE was separated by solid-phase extraction into hydrocarbon, ketone, and polar fractions using silica gel columns. The column was prepared in a Pasteur pipette with a DCM-treated glass wool plug and 0.5 g of silica gel (60 Å pore size, 70–230 mesh). Hydrocarbons were eluted from the column with 4 ml of hexane; ketone, ester, and aromatic compounds were eluted with 4 ml of dichloromethane; and polar compounds were eluted with 4 ml of methanol. The hydrocarbon fraction containing the *n*-alkanes was used for further analysis.

4.2.1. *n*-Alkane Quantification

n-Alkanes were analyzed on an Agilent 7890A GC equipped with both a mass selective detector (5975C MSD) and flame ionization detector at the Lamont-Doherty Earth Observatory Organic Geochemistry Laboratory. The oven temperature was set at 60 °C (1.5-min hold) ramped to 150 °C at 15 °C/min, then ramped to 320 °C at 4 °C/min and held for the duration of the analysis. *n*-Alkane abundances were quantified using the MSD peak area normalized to the 5 α -androstane internal standard. We corrected for molecular-dependent changes in ionization efficiency using a standard mixture of *n*C₈–*n*C₄₀ *n*-alkanes and 5 α -androstane that was analyzed repeatedly during the sample analyses.

4.2.2. Hydrogen and Carbon Isotope Measurements

Hydrogen and carbon isotope measurements were conducted in the Organic Geochemistry Laboratory at Lamont Doherty Earth Observatory on a Thermo DeltaV coupled to a Thermo Trace GC through a Thermo IsoLink and ConFlo IV. Eluting compounds were pyrolyzed to hydrogen gas at 1420 °C in an empty alumina tube conditioned with two 0.5- μ l aliquots of hexane (Burgoyne & Hayes, 1998). Evolved gases were introduced to the IRMS (isotope ratio mass spectrometer) through an open split in the ConFlo IV. A calibrated laboratory reference gas was injected at the beginning and end of each GC run and used to assess isotope drifts throughout the run. A molecular mixture with known isotopic values (Mix A5 supplied by Arndt Schimmelmann, University of Indiana) was injected between groups of 5–10 samples and used to correct the isotope values to the VSMOW (Vienna Standard Mean Ocean Water) scale.

To assess hydrogen isotope drift throughout the life of the reactor, a drift sample was run a few times at the beginning of a reactor and then between every five samples. We found that the isotopic values of a new reactor stabilize after ~5–10 injections. Throughout the sequence of analyses, the isotopic value of *n*C₂₉ and *n*C₃₁ in the drift sample was monitored and compared to their isotopic values at the beginning of the reactors life after the isotopic values had stabilized. Samples were corrected based on the trend of *n*C₂₉ and *n*C₃₁ δ D values in the drift sample from their stabilized isotopic value. An H₃⁺ factor determination was run between every 5–10 samples, and samples were corrected for H₃⁺ using the Isodat software (Sessions et al., 2001). Hydrogen samples were converted to the VSMOW scale using the average isotope values of all compounds in the Mix A5 standard (supplied by Arndt Schimmelmann, Indiana University, Bloomington, IN). The standard deviation of the mean of the reference gas molecules was larger than the analytical uncertainty (case 2 in Polissar & D'Andrea, 2014); therefore, laboratory reference gas uncertainty is quantified using the standard deviation of the means of the reference gas uncertainty (Table S1). For hydrogen, we used GC peak areas greater than 20 V/s (which corresponds to greater than ~200 ng per peak on our system). This minimum peak area cutoff was chosen because below this peak size there was an increasingly large size effect on peak δ D values.

For the plants, carbon isotopes were converted to VPDB scale using the average isotope values of all compounds in the Mix A4 standard (supplied by Arndt Schimmelmann, Indiana University, Bloomington, IN). Uncertainty was calculated the same way as hydrogen and GC peak sizes ranging 3–300 V/s were used, corresponding to 6 to 600 ng per peak (Table S1). For the soils, Mix A4 and Mix F8 were used to convert to VPDB scale. Only one GC analysis was made for each sample. Analytical uncertainty for these samples (0.35‰) was determined based on average results from a larger sample set analyzed at the same time as the soil samples.

Isotope ratios and analytical uncertainty were calculated using the method of Polissar and D'Andrea (2014). In short, the method calculates the measurements for isotope drifts throughout the life of the reactor,

converts the values to VSMOW or VPDB scales, and calculates the total uncertainty of the measurements including both analytical uncertainty and the uncertainty associated with realizing the VSMOW and VPDB scales.

4.3. Climate Data

4.3.1. Isotopic Composition of Rainfall

We used the weighted average isotopic composition of rainfall from Goldsmith et al. (2017; see paragraph 3.3) and added an additional site (Har Canaan) from the WISER database (http://www-naweb.iaea.org/napc/ih/IHS_resources_isohis.html, accessed September 2015).

4.3.2. Rainfall Amount

Average annual rainfall data (1981–2010) were acquired from the Israel Meteorological Service (<http://www.ims.gov.il/IMS/CLIMATE/ClimaticAtlas/RainNormals.htm>, accessed September 2015). Ten of the sites have rainfall stations within 5 km of the sampling locations. Data for Alon and Hermon were acquired from the Israel Rainfall Atlas (<http://www.ims.gov.il/IMS/CLIMATE/ClimaticAtlas/RainMaps.htm> accessed March 2016).

4.3.3. Temperature

The temperature data are from Goldsmith et al. (2017). We added one additional site (Har Canaan) from the Israel Meteorological Service database (<http://www.ims.gov.il/IMS/CLIMATE/ClimaticAtlas/TempNormals.htm>, accessed September 2015).

4.3.4. Relative Humidity

Monthly averages of hourly relative humidity (RH) from 1995 to 2009 were used for the analysis. The data were acquired from the Israel Meteorological Service (<http://www.ims.gov.il/IMS/CLIMATE/ClimaticAtlas/Relative+humidity+1995-2009.htm>, accessed March 2016). Seven of 12 sampling sites have a RH monitoring station in close proximity (<5 km). Four additional sites have RH monitoring station in a 20-km radius from them, located at similar elevation and longitude. One site (Alon) does not have RH data (see Table 1).

4.3.5. Potential Evapotranspiration and Aridity Index

Monthly and annual potential evapotranspiration (PET) data were extracted from Zomer et al. (2008) for each site. The aridity index (AI) was calculated as precipitation/PET.

Temperature, RH, PET, and AI data were averaged for each plant sample location based upon the flowering months (in the absence of data regarding leaf production months we assume that the flowering months are similar to leaf production months). Plants that were not identified were assigned December-January-February (DJF) data based upon the overall most common growing season in this region. The Hermon site is an exception because it is covered by snow most of the winter; we used FMA data for the growing season at this site.

5. Results

5.1. *n*-Alkane Concentration

n-Alkane distributions in soils and plants are characterized by an odd-over-even pattern with higher abundances of longer chain lengths, where nC_{31} and nC_{29} are the most abundant homologues. Total plant *n*-alkane concentrations (nC_{21} – nC_{37}) vary over 3 orders of magnitude (25,000–1,200,000-ng/g dry weight; Table S2-1). In general, C_3 plants have higher concentrations than C_4 plants. Total *n*-alkane concentrations (nC_{21} – nC_{37}) in the soils range from 3,500–23,000 ng/g and 450–2,200 ng/g in Mediterranean and desert soils, respectively. The differences between these soil groups is likely explained by both lower concentrations of C_3 versus C_4 and fewer plants on the landscape at the desert sites compared to the Mediterranean region.

5.2. *n*-Alkane Chain Length Distributions

5.2.1. Distributions of C_3 and C_4 Plants and Soils

We conducted a cluster analysis to understand the relationships between *n*-alkane distributions. We normalized the compound concentrations to a unit sum, performed hierarchical clustering using Euclidean distance, and present the results as a dendrogram for C_3 plants, C_4 plants, and soils (Figure 2 and Appendix C in the supporting information for plots of all samples). For each group in each dendrogram we created a boxplot showing the average chain length distributions (Figure 2).

Table 1
Sampling Site Data

Site		Coordinate		Elevation	Rainfall	DJF temperature	DJF PET	DJF RH	δD_r
Number	Name	N	E	(m asl)	(mm/year)	(K)	(mm per 3 moths)	(%)	(‰)
1	Hermon	33.27398	35.75821	1,337	1,300	278.1	102	72	-34.8
2	Har Canaan	33.02356	35.49748	858	671	281.9	115	77	-29.3
3	Peki'in	32.98272	35.3158	650	585	283.7	129	68	-29.3
4	Michmanim	32.88376	35.38066	157	590	284.3	159	68	-29.2
5	Haifa	32.79204	34.97167	102	539	287.1	158	66	-25.6
6	Beit Dagan	31.96735	34.90578	50	520	287.1	183	72	-18.6
7	Soreq	31.75327	35.02987	400	509	285.0	162	66	-22.4
8	Jerusalem	31.7857	35.17076	815	691	282.8	145	63	-28.1
9	Alon	31.80058	35.33009	290	400	285.9	172	NaN	-19.3
10	Arad	31.23727	35.21481	558	129	284.1	163	64	-14.4
11	Beer Sheva	31.24406	34.89974	353	195	285.7	174	68	-13.5
12	Mitzpe ramon	30.6199	34.7867	828	69	282.5	152	59	-13.6

Note. Abbreviations: DJF—December, January, and February growing months; PET—potential evapotranspiration; RH—relative humidity.

The C_3 plant dendrograms shows that they can be divided into three distinct groups based on their chain length distributions (Figure 2). The most abundant C_3 group, Type #1, is dominated equally by nC_{29} and nC_{31} , similar to distributions in woody angiosperms (Bush & McInerney, 2013). Group #2 is dominated by nC_{29} and group #3 by nC_{31} . The dendrogram groupings do not correlate with plant type, group, family, or growth habit. In some cases, plants of the same species sampled at different locations fall into different dendrogram groups.

The C_4 plant dendrogram shows that four of the five C_4 are plants characterized by high abundances of nC_{27} and nC_{29} (Group 2). This C_4 distribution differs from the higher abundances of nC_{31} – nC_{35} in African C_4 plants (e.g., Bush & McInerney, 2013; Garcin et al., 2014; Rommerskirchen et al., 2006; Vogts et al., 2012) and could reflect that these Israeli plants are C_4 dicots rather than the dominantly C_4 monocots in the African data set. Group 1 is only composed of the cactus *Opuntia ficus-indica*, which is a Crassulacean Acid Metabolism (CAM) plant that shows high abundance of nC_{33} and nC_{35} , similar to succulents described in Bush and McInerney (2013). While there is a need to investigate the CAM plants separately, as the $\delta^{13}C_{wax}$ and δD_{wax} of the single CAM plant that we analyzed fall within the range of the C_4 plants, we feel that for the purpose of this work it is reasonable to group the CAM with the C_4 plants.

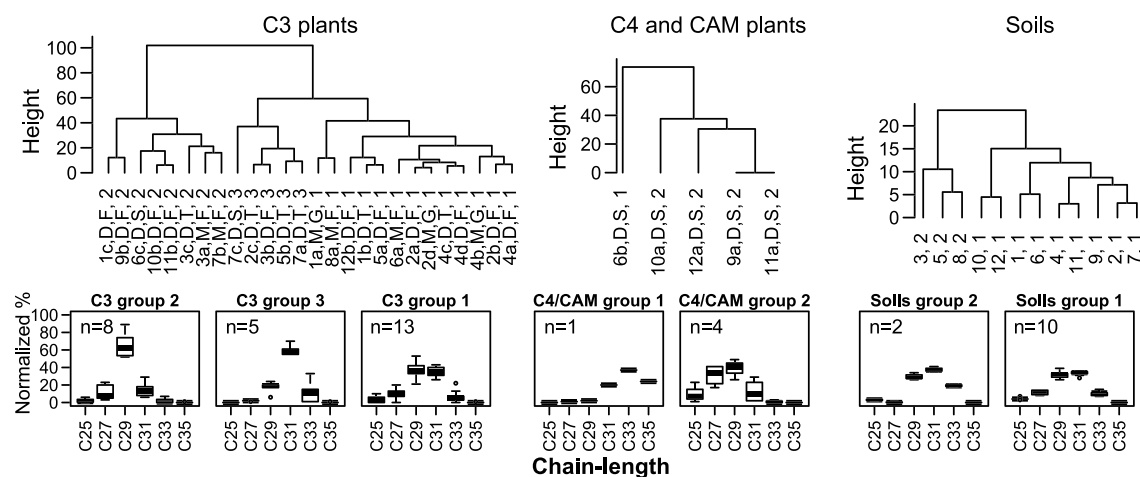


Figure 2. Top: dendrograms of C_3 and C_4 /CAM plants and soils. The notation below each branch represent site # (number) + plant # (letter), + Dicot/Monocot, + growth form (Forb, Shrub, Tree, and Graminoid), + group number (number; e.g., “1c, D, F, 2” is site number 1 (Hermon), c is the third plant in site 1; it is a Dicot Forb and is in group number 2). Bottom: chain length distribution of each of C_3 and C_4 /CAM plants and soils groups.

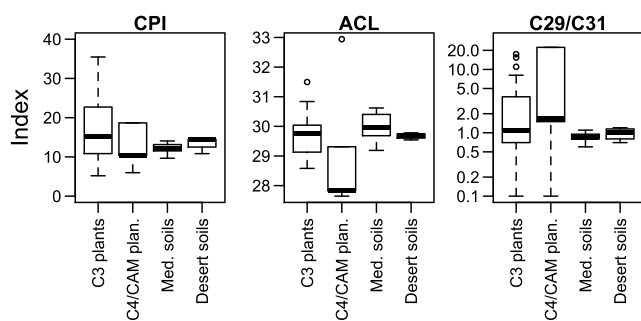


Figure 3. Boxplot of CPI, ACL, and nC_{29}/nC_{31} (note log scale for y axis in nC_{29}/nC_{31} plot) showing median (bold line), middle quartiles (box), range (vertical dashed lines), and outliers (open circles) of C_3 and C_4 plants and Mediterranean and desert soils.

three chain length distribution indexes was evaluated for C_3 plants, C_4 plants, Mediterranean soils, and desert soils. The CPI is overall high and not systematically different between any of these groups; however, within group variability it is greatly reduced in the soils compared to the plants (Figure 3). The results that describe chain lengths (ACL and nC_{29}/nC_{31}) reinforce the groupings exhibited in the dendrogram analysis (Figure 3): C_4 plants have lower ACL and higher nC_{29}/nC_{31} compared to C_3 plants, while the soils are more similar to the C_3 rather than the C_4 plants. Within group variability of the soils is also greatly reduced for ACL and nC_{29}/nC_{31} (Table 2).

5.3. Plant and Soil $\delta^{13}C_{wax}$

5.3.1. $\delta^{13}C_{wax}$ Results

Plant nC_{29} $\delta^{13}C_{wax}$ show values typical for C_3 ($-34.0 \pm 2.2\%$, range: 8.6%, $n = 26$) or C_4 ($-22.6 \pm 1.3\%$, range: 3.5%, $n = 5$) values (Figure 4, Tables 2 and S2-3, Figure S13, and Appendix C in the supporting information for plots of all samples). These values are essentially identical to the Tipple and Pagani (2010) mean values of C_3 -33.1‰ and C_4 -21.7‰, once $\delta^{13}C_{wax}$ is corrected for a -0.7% change in atmospheric $\delta^{13}C$ of CO_2 (-7.8% in Tipple & Pagani, 2010, versus -8.5% in 2014—from Scripps CO_2 program: <http://scrippsco2.ucsd.edu/>, accessed February 2018). The $\delta^{13}C_{wax}$ values of C_3 plants are similar across different growth forms (Figure S13). The Mediterranean soils have an average of $-35.6 \pm 0.4\%$ and a range of 1.1‰ (Figure 4 and Table 2). The desert soils have an average of $-33.4 \pm 0.5\%$ and a range of 1.1‰ (Figure 4 and Table 2).

Plant $\delta^{13}C_{wax}$ homologues are highly correlated with each other (r^2 values from 0.5 to 0.9 Table S2-2), while soil $\delta^{13}C_{wax}$ homologues are only weakly correlated (Table S2-2). Soil $\delta^{13}C_{wax}$ variability of all homologues is greatly diminished with respect to plant $\delta^{13}C_{wax}$. In the Mediterranean area that only contains C_3 plants, the range of soil $\delta^{13}C_{wax}$ is tenfold smaller than that of the plants, indicating that homogenization during the integration process of plant alkanes into soil is an extremely efficient process and possibly the sourcing and mixing of plants into soil mixtures is similar between sites. We do not find an enrichment of soil $\delta^{13}C_{wax}$ when compared to plant $\delta^{13}C_{wax}$ as has been suggested previously (Chikaraishi & Naraoka, 2006; Nguyen Tu et al., 2004).

The $\delta^{13}C$ of the nC_{27} homologue is more positive than other homologues in both desert and Mediterranean soils. In our data set, C_4 plants have more abundant nC_{27} than C_3 plants; therefore, more enriched nC_{27} values could reflect increased contributions from C_4 plants to the nC_{27} homologue. While this explanation may be correct for desert soils where C_4 vegetation is present, many of the Mediterranean sites do not have any C_4 plants present. Additional sources of n -alkanes not measured here, such as soil microbes, could contribute to shorter homologues, and it remains uncertain why the Mediterranean soils have more enriched nC_{27} homologues.

5.4. Plant and Soil δD_{wax}

5.4.1. δD_{wax} Results

Plant δD_{wax} shows a range of $\sim 100\%$ along a 20‰ δD_r rainfall gradient (Figure 5a). Such a large range agrees with previous published data (Berke et al., 2015; Sachse et al., 2012), underscoring the complex processes

The soils dendrogram shows that all soil distributions are highly similar compared to the plants (maximum distance ~ 20 compared to >60), and the two major groups (which would be grouped together in the plants analysis) are both dominated equally by nC_{29} and nC_{31} . The boxplot shows that variability in the normalized chain length distribution of soils is small, as expected from the clustering dendrogram. The soil chain length distribution is similar to the chain length distribution of Group #1 in the C_3 plants.

5.2.2. Chain Length Distribution Indexes

Indices that describe the distribution of n -alkane homologues provide a simplified means to summarize such distributions. Here we examine the commonly used average chain length (ACL) and carbon preference index (CPI; using equations from Tipple & Pagani, 2013). In addition, we also evaluated the nC_{29}/nC_{31} ratio, which are the key homologues driving the changes in the dendrograms in Figure 2. The distribution of these

Table 2
Statistical Parameters of Variability for ϵ_{app} , $\delta^{13}C_{wax}$, CPI, ACL, and nC_{29}/nC_{31} of C_3 and C_4 Plants and Mediterranean and Desert Soils

	$nC_{29} \delta^{13}C$				CPI				ACL				C_{29}/C_{31}							
	mean	s.e.m	stdev	range	mean	s.e.m	stdev	range	mean	s.e.m	stdev	range	mean	s.e.m	stdev	range				
C_3 plants	-138	3.9	20.1	77	-34.0	0.4	2.2	8.6	18.6	2.2	11.2	49.2	29.7	0.1	0.7	2.9	2.6	0.9	3.6	15.3
C_4 plants	-118	18.1	36.1	80	-22.6	0.6	1.3	3.5	18.4	7.4	16.4	40.7	29.1	1.0	2.2	5.3	9.6	5.2	11.6	22.2
Med soils	-124	2.3	6.8	16	-35.6	0.1	0.4	1.1	12.1	0.5	1.4	4.4	30.0	0.2	0.5	1.4	0.9	0.1	0.2	0.5
Desert soil	-123	6.8	13.7	30	-33.4	0.3	0.5	1.1	13.5	0.9	1.8	3.7	29.7	0.1	0.1	0.2	1.0	0.1	0.2	0.5

involved in the fractionation process (Sachse et al., 2012). Partitioning the data based upon growth habit shows that trees group in a relatively narrow range (~30‰), while shrubs, forbs, and graminoids show a much larger range (Figure 5a).

Soil δD_{wax} shows a range of 40‰ although excluding the driest site decreases the range to 15‰ and 20‰ for nC_{29} and nC_{31} , respectively. This range is almost an order of magnitude smaller than the range of plant δD_{wax} and is similar to the range of δD_r . Soil δD_{wax} values fall within the range of plant δD_{wax} (Figure 5b). These results differ from previous studies that find that soil δD_{wax} is depleted from that of plants (Chikaraishi & Naraoka, 2006).

There is a high correlation between plant δD_{wax} , nC_{27} , nC_{29} , and nC_{31} homologues ($r^2 > 0.8$; Table S2-3). Plant δD_{wax} , nC_{33} is correlated with the other three homologues albeit to a lesser degree ($r^2 > 0.45$; Table S2-3). The correlation between soil δD_{wax} homologues is lower than that of the plants (r^2 from 0.5 to 0.75; Table S2-3). This suggests that the isotopic composition of the different homologues in individual plants is derived from the same isotopic hydrogen pool, whereas soil δD_{wax} is an integration of many plants with different chain length distributions, decreasing the correlation between homologues.

6. Discussion

6.1. Environmental Controls on $\delta^{13}C_{wax}$

To test the possible environmental control on $\delta^{13}C_{wax}$ of C_3 and C_4 plants and soils, homologues nC_{27} through nC_{33} were regressed against annual rainfall, DJF temperature, DJF relative humidity, and relative humidity of flowering months. No significant correlation was found between plant or soil $\delta^{13}C_{wax}$ and any of these parameters (Table S2-2). These results indicate that in areas that contain only one growing season, the major process affecting $\delta^{13}C_{wax}$ is the photosynthetic pathway and that even in these areas plant $\delta^{13}C_{wax}$ variability is still large. The large plant $\delta^{13}C_{wax}$ variability indicates that there are probably additional minor microenvironmental processes (e.g., slope, shade cover, size, and depth of roots) or differences in the fractionation between leaf $\delta^{13}C$ and $\delta^{13}C_{wax}$ affecting the isotopic value. Soil $\delta^{13}C_{wax}$ shows a near-constant value of $-35.6\text{‰} \pm 0.4\text{‰}$ in the Mediterranean region that spans an 800-mm/yr rainfall gradient and shows no correlation with environmental parameters.

In the desert region that contains both C_3 and C_4 plants, soil $\delta^{13}C_{wax}$ is enriched compared to the Mediterranean soils. Surprisingly, soil $\delta^{13}C_{wax}$ in the desert region is more depleted (~2‰) than any of the C_3 plants sampled there. The reason for this is unclear. One possibility is that there have been changes in vegetation at the sites and the vegetation we sampled does not reflect the time-integrated contributions to the soils. Another option is that the agricultural terraces were used to grow C_3 plants (e.g., wheat and barley); and therefore, the soil $\delta^{13}C_{wax}$ is a mixture of modern and ancient vegetation. Radiocarbon dating of the soil organic matter and *n*-alkanes could potentially address this question but is beyond the scope of this study.

It has been suggested (Diefendorf et al., 2010; Kohn, 2010; Kohn, 2016) and debated (Schubert & Jahren, 2012) that bulk $\delta^{13}C$ ($\delta^{13}C_p$) in C_3 plants and organic matter in soils responds to mean annual precipitation. Thus, it is of interest to evaluate whether soil $\delta^{13}C_{wax}$ responds in a similar manner. Diefendorf et al. (2010) showed a logarithmic relation between carbon isotope discrimination (ϵ_{leaf} , the difference between plant $\delta^{13}C$ and $\delta^{13}C$ in atmospheric CO_2 ; Farquhar et al., 1989) in C_3 plants and mean annual precipitation:

$$\epsilon_{leaf} = 5.54(\pm 0.22) \times \log_{10}(\text{MAP}) + 4.07(\pm 0.7) \quad (1)$$

where MAP is mean annual precipitation, the standard error is in parentheses, and ϵ_{leaf} is (after Farquhar et al., 1989):

$$\epsilon_{leaf} = (\delta^{13}C_{CO_2} - \delta^{13}C_p) / (1 + \delta^{13}C_p / 1,000) \quad (2)$$

where $\delta^{13}C_{CO_2}$ is $\delta^{13}C$ in atmospheric CO_2 . We used the 2014 $\delta^{13}C_{CO_2}$ value of -8.4‰ (Keeling et al., 2010, <http://scrippsco2.ucsd.edu/>, accessed, 5, 2019).

To compare our results of soil $\delta^{13}C_{wax}$ versus mean annual rainfall with the Diefendorf et al. (2010) relationship, we converted $\delta^{13}C_p$ in their model to $nC_{29} \delta^{13}C_{wax}$ using (after Chikaraishi et al., 2004)

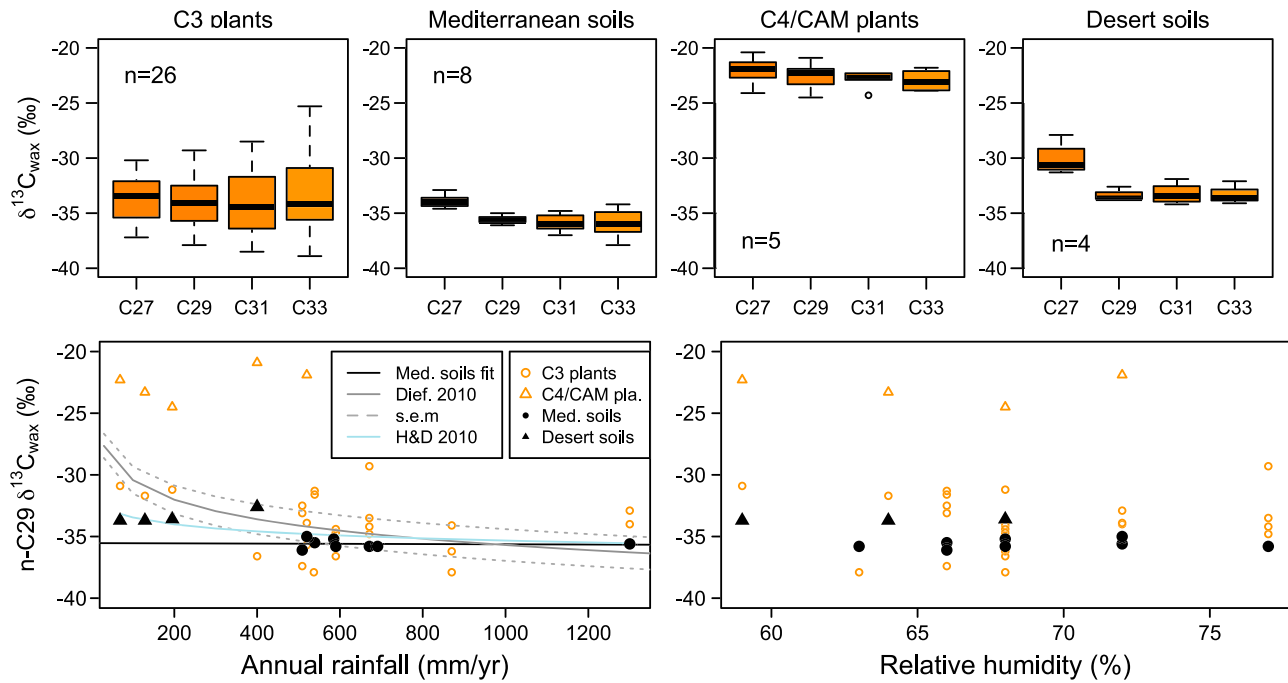


Figure 4. Top: Boxplot of $n_{C_{27}-n_{C_{33}}} \delta^{13}C_{wax}$ for C_3 plants, Mediterranean soils, C_4 plants, and desert soils. Bottom, left: correlation between $n_{C_{29}} \delta^{13}C_{wax}$ and mean annual rainfall, linear trend line for Mediterranean soil $n_{C_{29}} \delta^{13}C_{wax}$ (black line), and predicted angiosperm and standard error (dashed line) for $n_{C_{29}} \delta^{13}C_{wax}$ using the relation between bulk $\delta^{13}C$ and mean annual rainfall (Diefendorf et al., 2010) converted to $n_{C_{29}} \delta^{13}C_{wax}$ assuming a constant offset with bulk tissue values (Diefendorf & Freimuth, 2017; gray lines). The blue line is the predicted $n_{C_{29}} \delta^{13}C_{wax}$ using the Hartman and Danin (2010) bulk plant $\delta^{13}C$ trend line extrapolated over the full range. Bottom, right: correlation between $n_{C_{29}} \delta^{13}C_{wax}$ and relative humidity.

$$\epsilon_{p-wax} = [(\delta^{13}C_{wax} + 1,000)/(\delta^{13}C_p + 1,000) - 1] \times 1,000. \quad (3)$$

As the majority of our plants are shrubs and forbs, we used a fractionation factor (ϵ_{p-wax}) of -7.4% (Diefendorf & Freimuth, 2017).

We also evaluated the relationship in Israel between $\delta^{13}C_p$ and mean annual precipitation using the $\delta^{13}C_p$ data measured along a similar transect in Israel (Hartman & Danin, 2010). We replotted the original data and converted it to $\delta^{13}C_{leaf}$ (Farquhar et al., 1989) using the 2007 (original year of sampling) $\delta^{13}C_{CO_2}$ value of -8.1% (Keeling et al., 2010) and calculated the trend line of the data ($R^2 = 0.36$, $p < 0.005$):

$$\delta^{13}C_{leaf} (\text{Israel}) = -0.86 \cdot \ln(\text{MAP}) + 14.37 \quad (4)$$

where MAP is mean annual precipitation. To compare Hartman and Danin (2010) data to ours, we converted $\delta^{13}C_{leaf} (\text{Israel})$ to $\delta^{13}C_p$ using the 2014 $\delta^{13}C_{CO_2}$ value and converted it to angiosperms $\delta^{13}C_{wax}$ using equation (3).

Figure 4 shows the Diefendorf et al. (2010) and Hartman and Danin (2010) trend lines converted to $\delta^{13}C_{wax}$. Over the rainfall range of the Mediterranean sites (1,300–500 mm/year) the Diefendorf et al. (2010) data span $\sim 2\%$, whereas the Hartman and Danin (2010) data span $\sim 0.8\%$.

Comparing the measured Mediterranean soil $\delta^{13}C_{wax}$ and $\delta^{13}C_{wax}$ predicted from the Diefendorf et al. (2010) and Hartman and Danin (2010) $\delta^{13}C_p$ relationships shows that soil $\delta^{13}C_{wax}$ along the presented transect does not respond to changes in mean annual rainfall as does $\delta^{13}C_p$.

Plant and soil $\delta^{13}C_{wax}$ of both C_3 and C_4 plants are also not correlated with rainfall, growing season temperature, or elevation. There are two options to explain this observation. The first and more plausible is that a significant portion of the growth phase occurs during the rainy season, and therefore, there is no water stress/aridity effect (see Tipple et al., 2013, for similar results for δD_{wax}). The second is that plant $\delta^{13}C_{wax}$

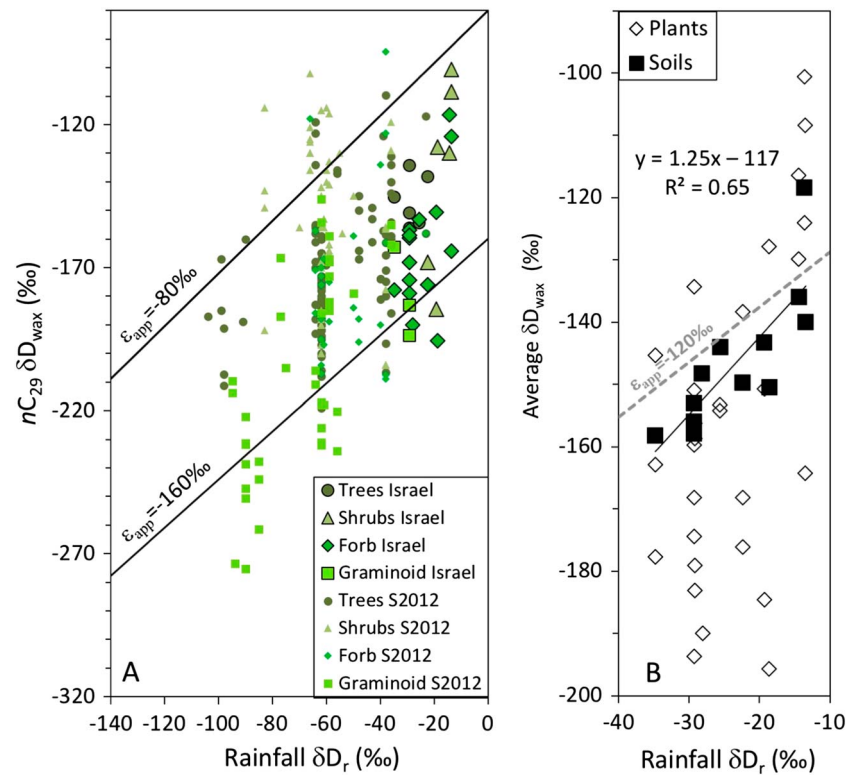


Figure 5. (a) Compilation of plant $nC_{29} \delta D_{wax}$ versus δD_r ; larger symbols indicate plants measured in this research, and smaller borderless symbols are from Sachse et al. (2012). Apparent fractionation factors of -80‰ and -160‰ are added for context (black lines; see paragraph 6.2.1 for details). (b) Plant (diamond) and soil (square) average δD_{wax} versus δD_r from the Israel transect. Apparent fractionation of -120‰ is provided for context (gray dashed line).

is not affected by water stress. We favor the first option based on prior research showing that regions with more than one rainy season show a small water stress effect (Garcin et al., 2014; Schwab et al., 2015).

It has been suggested that soil $\delta^{13}C_{wax}$ reflects the relative proportions of C_3 versus C_4 plants on the landscape (e.g., Lichtfouse et al., 1994; Lichtfouse et al., 1997) and is thus a proxy for these proportions on ancient landscapes (e.g., Ficken et al., 1998; Magill et al., 2013; Uno et al., 2016). Our results show that soil $\delta^{13}C_{wax}$ in exclusively C_3 plant habitats is insensitive to rainfall amount, unlike bulk leaf tissue. Therefore, soil $\delta^{13}C_{wax}$ should be unaffected by the uncertainty due to possible changes in rainfall amount that affects bulk $\delta^{13}C$. This suggests that soil $\delta^{13}C_{wax}$ is possibly a better recorder of C_3/C_4 plants on the landscape than bulk $\delta^{13}C$. However, as our soil $\delta^{13}C_{wax}$ data from the desert soils show a pure C_3 signal (see discussion above), we cannot use these data to validate this suggestion. The soil leaf wax pool reflects the flux-weighted composition of different sources that could also affect how C_3/C_4 contributions are recorded (see section 6.4). Further calibration work will be needed to substantiate this observation.

6.2. Environmental Controls on δD_{wax}

Prior studies have shown that δD_{wax} is primarily governed by the isotopic composition of rainfall (δD_r), evaporation and evapotranspiration, and vegetation type (Sachse et al., 2012). To test the possible environmental control on plant and soil δD_{wax} , the δD of nC_{27} – nC_{33} were regressed against δD_r , annual rainfall amount, DJF temperature, DJF relative humidity, relative humidity of flowering months, and potential evapotranspiration during the growing months. δD_{wax} values of C_3 plants do not show significant correlation to any of these parameters. Some of the δD_{wax} homologues of C_4 plants show a correlation (albeit $p < 0.1$) with some of these parameters (Table S2-3), most noteworthy is nC_{31} that shows a significant correlation with δD_r , annual rainfall, and DJF RH. However, these results should be considered tentative as only five C_4 plants were sampled.

Soil δD_{wax} shows significant correlation ($p < 0.1$) with δD_r for nC_{27} , nC_{29} , and nC_{31} ($r^2 = 0.64, 0.3$, and 0.31 , respectively), with relative humidity for nC_{27} , nC_{29} , and nC_{31} ($r^2 = 0.69, 0.43$, and 0.43 , respectively), while annual rainfall amount shows significant correlation with nC_{27} and nC_{31} ($r^2 = 0.53$ and 0.3 , respectively; Table S3). The slope of the correlation between soil δD_{wax} and δD_r is 1.25, which is larger than expected (e.g., for $\epsilon_{app} = -120\%$ and -140% , the expected slope would be 0.88 and 0.86, respectively; Polissar & Freeman, 2010) and will be discussed in paragraph 6.2.1. Winter temperatures do not show any correlation with any of the homologues. The soil samples were further divided into Mediterranean and desert sites, and soil δD_{wax} from each region was evaluated against the above parameters. For the individual groups, none of the homologues show a significant correlation with any of the environmental parameters.

It has been proposed that averaging the isotopic composition of the various homologues results in better correlation with environmental parameters (e.g., Feakins & Sessions, 2010; Kahmen et al., 2013). We examined three δD_{wax} averaging methods: (a) average δD_{wax} of odd nC_{25} – nC_{35} , (b) amount-weighted average δD_{wax} of odd nC_{25} – nC_{35} , and (c) amount-weighted average δD_{wax} of odd C_{27} – C_{31} (after Feakins & Sessions, 2010). Average soil δD_{wax} using the three averaging methods are significantly correlated ($p < 0.03$) with δD_r ($r^2 = 0.64, 0.40$, and 0.34 , respectively), annual rainfall ($r^2 = 0.61, 0.38$, and 0.44 , respectively), and DJF RH ($r^2 = 0.55, 0.49$, and 0.44 ; Table S2-3). Of the three averaging methods, the unweighted average shows the highest correlations. Average plant δD_{wax} using the three averaging methods is not significantly correlated with any of the environmental parameters. When separating the soils into Mediterranean and desert soils, the correlation with environmental parameters becomes nonsignificant, regardless of the averaging method.

We further tested the unweighted average method on soil δD_{wax} from Schwab et al. (2015) and found that average δD_{wax} over a series of homologues results in a better correlation than each individual homologues (raising the r^2 from 0.68 to 0.77). These results indicate that for soil δD_{wax} , the unweighted averaging method produces the best correlation with δD_r .

6.2.1. Apparent Fractionation

To further the understanding of the processes affecting δD_{wax} , we assessed the apparent fractionation factor ($\epsilon_{app} = (\delta D_{wax} + 1)/(\delta D_r + 1) - 1$), which is the depletion of δD_{wax} with respect to δD_r (Sachse et al., 2012) against environmental parameters. In general, plant ϵ_{app} is more negative in areas with higher RH and lower evapotranspiration rates and varies as a function of plant type (Sachse et al., 2012). In this compilation of plant ϵ_{app} , the range in values is $\sim 100\%$ (Sachse et al., 2012). In lake sediments, the range is on the order of 35% (e.g., Garcin et al., 2012; Hou et al., 2008; Polissar & Freeman, 2010). Though, ecosystem-specific ϵ_{app} can have smaller ranges of 5 – 20% (Polissar & Freeman, 2010).

The average ϵ_{app} of C_3 plants in the Israel transect is $-138 \pm 20\%$ (1σ and throughout) and $-140 \pm 28\%$ for nC_{29} and nC_{31} , respectively (Figure 6). Partitioning the data based on growth form (Figure S13) shows that C_3 trees have the smallest ϵ_{app} and C_3 graminoids the largest (similar to results in Sachse et al., 2012), where forbs span the full range and shrubs cannot be evaluated due to small sample size ($n = 2$). For C_4 plant, the average ϵ_{app} is $-117 \pm 36\%$ and $-115 \pm 24\%$ for nC_{29} and nC_{31} , respectively (Figures 6 and S13).

Soil average ϵ_{app} is $-124 \pm 8\%$ and $-127 \pm 7\%$ for nC_{29} and nC_{31} , respectively (Figure 6). The Mediterranean soils and the desert soils show similar ϵ_{app} values, with an average of both Mediterranean and desert soils of $\epsilon_{app} = -126 \pm 7\%$ (based on the average and 1σ of the ϵ_{app} , Table S2-3). The range of soil ϵ_{app} is $\sim 20\%$ and $\sim 25\%$ for the Mediterranean and desert soils, respectively, which is an 80% reduction compared to plant ϵ_{app} .

Average soil ϵ_{app} shows a significant correlation with RH ($r^2 = 0.55$, $p = 0.009$; Figure 6), where smaller soil ϵ_{app} occur in areas with lower RH. These results agree with previous work (e.g., Sachse et al., 2012). Soil ϵ_{app} does not show a significant correlation with annual rainfall (Figure 6), PET (annual or winter), and P-PET (not shown).

Soil average δD_{wax} is significantly correlated with both δD_r and RH, and soil ϵ_{app} is correlated with RH. The correlation between δD_{wax} and both δD_r and RH can explain the higher than expected slope of soil δD_{wax} versus δD_r (Figure 5b). In Israel, RH, δD_r , and rainfall amount are all correlated (Table S2-3); therefore, the effect of RH on ϵ_{app} amplifies the δD_{wax} slope with respect to δD_r (i.e., in dry areas, δD_r starts off more enriched and because RH is lower, evaporative enrichment is higher, thus resulting in a larger slope and

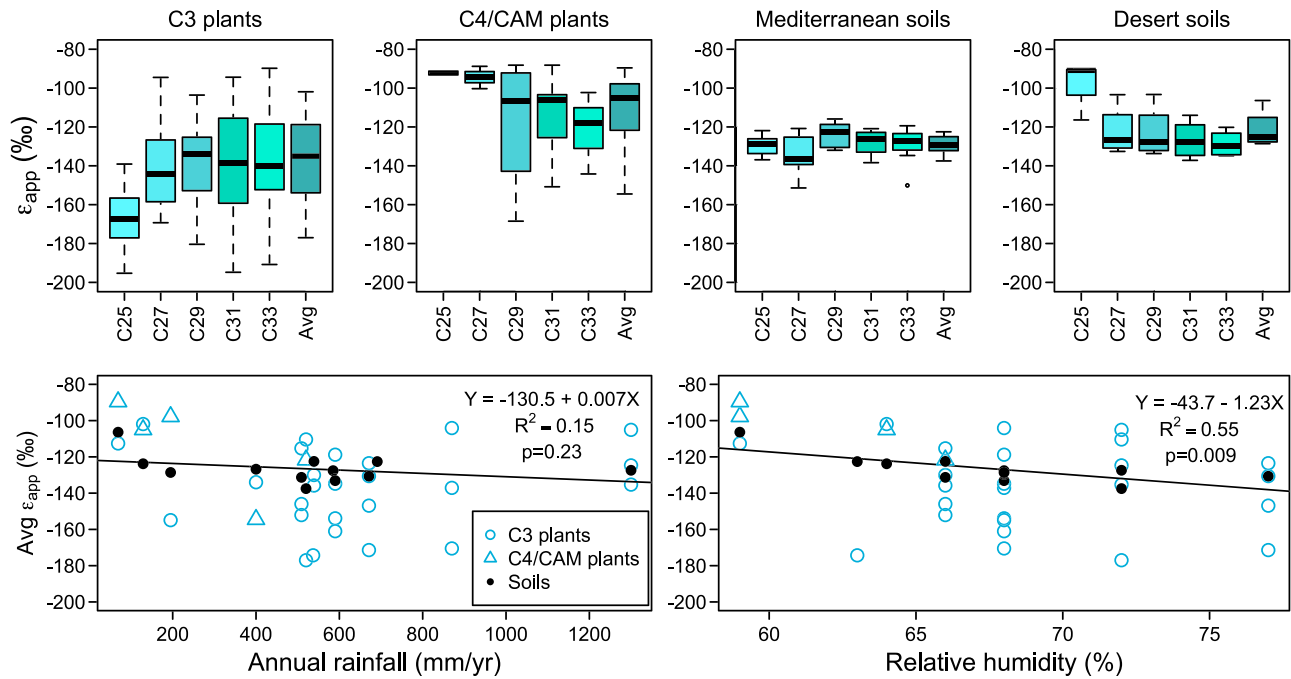


Figure 6. Top: Boxplot of C_{25} - C_{33} and homologues average ϵ_{app} for C_3 and C_4 plants and Mediterranean and desert soils (y axes are same for all plots). Bottom, left: Plant and soil homologues average ϵ_{app} versus rainfall and bottom, right: versus relative humidity. Linear trend lines were fit to the soil data (black lines; y axes are same for both plots).

an enrichment of δD_{wax} versus δD_r). To evaluate the combined dependence of δD_r and RH on δD_{wax} , a multiple linear regression was computed. The resultant empirical multiple linear regression equation is

$$avg\delta D_{wax} = -66.4 + 0.8 \times \delta D_r - 0.9 \times RH \quad (5)$$

where δD_r is in permil and RH is in percent. An alternate equation that uses the definition of ϵ_{app} and its relationship to RH (Figure 6) is

$$avg\delta D_{wax} = (\delta D_r + 1)(1.044 - 0.00123 \times RH) - 1 \quad (6)$$

where δD values are expressed without the 10^3 factor and RH is in percent units.

The multiple regression shows a better correlation ($r^2 = 0.73$, $p = 0.05$) than for each individual parameter and has a standard mean error of 6.9‰, indicating that both δD_r and RH effect $avg\delta D_{wax}$. The knowledge of the local RH can potentially improve the ability to determine ϵ_{app} and could reduce the uncertainty of reconstructing δD_r from $avg\delta D_{wax}$.

6.2.2. Seasonality of Leaf Production

Differences in seasonality of rainfall and leaf production have been proposed as one of the main reasons for δD_{wax} variability (e.g., Berke et al., 2015; Freimuth et al., 2017; Schwab et al., 2015). To assess the possible role of seasonality of leaf production, we divided the plants into two groups: C_3 plants that grow during the rainy season (JFMA - January, February, March, April, $n = 15$) and C_3 plants that grow after the rainy season (not JFMA, $n = 10$; Figure 7; see paragraph 4.1 for details). The contribution of seasonality to C_4 plants could not be assessed due to the small sample size of C_4 plants. We used the Mann Whitney U test to assess whether the ϵ_{app} of $n-C_{27}$, $n-C_{29}$, $n-C_{31}$, $n-C_{33}$, and average ϵ_{app} of plants that grew during the rainy season and those that grew after the rainy season are significantly different from one another.

The data suggest that plants that grow during the rainy season (-159% , -134% , -143% , -138% , -135% for of $n-C_{27}$, $n-C_{29}$, $n-C_{31}$, $n-C_{33}$, and average ϵ_{app}) have larger ϵ_{app} than plants that grow after the rainy season (-133% , -133% , -134% , -137% , -135% for of $n-C_{27}$, $n-C_{29}$, $n-C_{31}$, $n-C_{33}$, and average ϵ_{app} ; Figure 7). However, a Mann Whitney U test on these groups indicates that ϵ_{app} of C_3 rainy season and C_3 after rainy

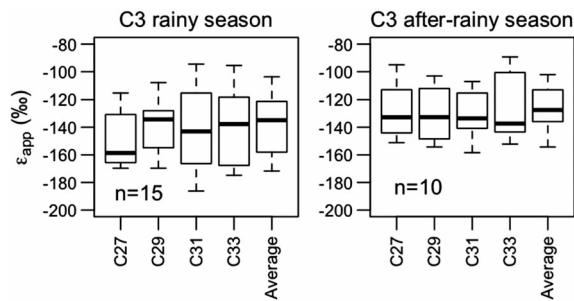


Figure 7. Boxplot of ϵ_{app} of nC_{27} - nC_{33} and homologues average ϵ_{app} showing C_3 plants that grow during the rainy season and C_3 plants that grow after the rainy season.

season are not significantly different at the 0.95 level (p value of 0.1, 0.3, 0.4, 0.4, and 0.2 for nC_{27} , nC_{29} , nC_{31} , nC_{33} , and average ϵ_{app} , respectively). Therefore, although the measured difference between average ϵ_{app} of C_3 plants growing during the rainy season and after the rainy season is slightly negative, the contribution of seasonality to the total variability is not statistically significant.

6.3. Environmental Control on Chain Length Distributions

To test the possible environmental control on chain length distributions, CPI, ACL, and nC_{29}/nC_{31} were regressed against annual rainfall, DJF temperature, and DJF relative humidity. The results show that CPI, ACL, and nC_{29}/nC_{31} are not significantly correlated with any of these environmental parameters at a 95% confidence level. At a 90% confidence level, CPI values of Mediterranean, desert, and all soils are correlated with

annual rainfall ($r^2 = 0.39, 0.82,$ and $0.3,$ respectively). nC_{29}/nC_{31} of Mediterranean and desert soils are correlated with annual rainfall ($r^2 = 0.39$ and $0.94,$ respectively), though the combined soils show no relation.

In summary, we found that chain length distributions differ between C_3 and C_4 plants and that soil distributions were more similar to those of C_3 plants. No strong correlation was found between indices of chain length distribution (ACL and CPI) and environmental variables. These findings suggest that chain length distributions cannot easily be used to infer past environmental conditions but may have some taxonomic utility in understanding past vegetation types. As discussed below, the differences between plant types are also important for interpreting compound-specific isotope signatures of plant-wax mixtures such as occur in soils.

6.4. Incorporation of Plant δD_{wax} and $\delta^{13}C_{wax}$ Into Soils

Incorporation of unaltered plant wax n -alkanes into soils would produce a biomass weighted averaging of their isotopic and chain length distributions (i.e., the sum of the isotopic composition or chain length of each leaf produced multiplied by its weight divided by the weight of the total leaf biomass). However, the extent of preservation of the plant values throughout the incorporation into soils is unclear (Howard et al., 2018; Huang et al., 1997; Lichtfouse et al., 1994; Lichtfouse et al., 1997; Mazeas et al., 2002; Nguyen Tu et al., 2004; Nguyen Tu et al., 2011; Pond et al., 2002; Wiesenberg et al., 2004).

A comparison of long-chain n -alkanes from plants and soils shows a large decrease in concentration during the plant incorporation into soil (Chikaraishi & Naraoka, 2006; Mazeas et al., 2002; Nguyen Tu et al., 2004; Nguyen Tu et al., 2011; Zech et al., 2011); however, it is unclear whether this is a result of biodegradation or dilution of the n -alkanes in the soils (Chikaraishi & Naraoka, 2006). Likewise, the effect of degradation on plant δD_{wax} and $\delta^{13}C_{wax}$ is unclear. Some studies find little or no indication of isotopic modification during incorporation into soils (Huang et al., 1997; Mazeas et al., 2002; Pond et al., 2002; Zech et al., 2011), while others found that soil $\delta^{13}C_{wax}$ is enriched (Chikaraishi & Naraoka, 2006; Feakins et al., 2018; Nguyen Tu et al., 2004) or depleted (Wiesenberg et al., 2004) with respect to plant isotopic values.

We find that both soil δD_{wax} and $\delta^{13}C_{wax}$ fall within the range of plant δD_{wax} and $\delta^{13}C_{wax}$ (excluding $\delta^{13}C_{wax}$ from the desert soils), albeit with a much smaller range of values (Figure 8). In addition, we find that soil δD_{wax} significantly correlates with rainfall δD_r and that soil $\delta^{13}C_{wax}$ (in the Mediterranean sites) show values that are reasonable for a landscape containing only C_3 plants. Our results are thus consistent with a scenario in which soil δD_{wax} and $\delta^{13}C_{wax}$ form as a result of a biomass weighted averaging of plant-wax n -alkanes. However, as we did not conduct a long term, comprehensive study on the plant communities, we cannot quantitatively assess whether true biomass averaging is solely responsible for the soil δD_{wax} and $\delta^{13}C_{wax}$. Additionally, while our results cannot exclude the possible addition of long-chain n -alkanes from a microbial source, if present, this source must have δD and $\delta^{13}C$ values that reflect rainfall δD_r and characteristic C_3 plants and therefore have minimal impacts on the soil values.

6.5. Application of Soil δD_{wax} and $\delta^{13}C_{wax}$ for Paleoclimate Studies

Soil δD_{wax} and $\delta^{13}C_{wax}$ from paleosols (e.g., Magill et al., 2013; Uno et al., 2016) and sediments in archaeological sites (Patalano et al., 2015; Shelach-Lavi et al., 2019) are potential archives of local terrestrial

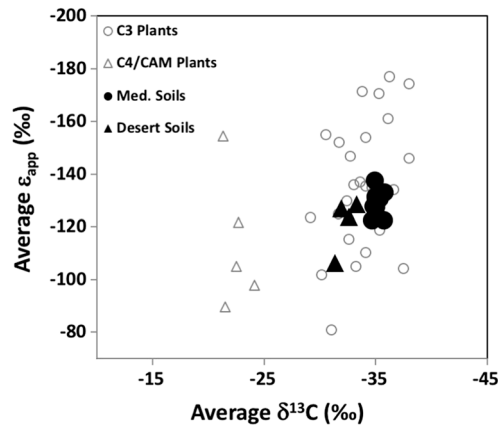


Figure 8. Average $\delta^{13}\text{C}_{\text{wax}}$ versus average ϵ_{app} , showing plant variability and the substantial reduction of variability from plants to soils in both parameters.

paleoclimate, which can substantially increase the spatial resolution of paleoclimate reconstructions. A fundamental question is whether plant $\delta\text{D}_{\text{wax}}$ and $\delta^{13}\text{C}_{\text{wax}}$ are averaged in soils to an extent that reduces the variability exhibited by individual plants and therefore allows a meaningful reconstruction of past climate (Chikaraishi & Naraoka, 2006; Graham et al., 2014; Nguyen Tu et al., 2011; Zech et al., 2011). Quantifying the uncertainty of these archives will enable researchers to reconstruct δD_r (and possibly rainfall amount) and the landscape C_3/C_4 ratio. Here we quantify the variability of soil $\delta\text{D}_{\text{wax}}$ and $\delta^{13}\text{C}_{\text{wax}}$ and assess the magnitude of homogenization in the plant-to-soil integration process.

Variability in soil $\delta^{13}\text{C}_{\text{wax}}$ ($0.4\text{‰ } 1\sigma$) across the Mediterranean sites is reduced by $\sim 80\%$ compared to variability in plant $\delta^{13}\text{C}_{\text{wax}}$ ($2.2\text{‰ } 1\sigma$; Figure 8 and Table 2). The soil $\delta^{13}\text{C}_{\text{wax}}$ is constant ($0.4\text{‰ } 1\sigma$) across a 800-mm/year rainfall gradient and thus appears insensitive to rainfall amount, in contrast to bulk plant leaf $\delta^{13}\text{C}$. If supported by other studies, this invariance holds promise for more accurate reconstructions of landscape C_3/C_4 from $\delta^{13}\text{C}_{\text{wax}}$.

For $\delta\text{D}_{\text{wax}}$, variability in soil $\text{avg}\epsilon_{\text{app}}$ ($7\text{‰ } 1\sigma$) across all sites is reduced by $\sim 70\%$ compared to plant $\text{avg}\epsilon_{\text{app}}$ variability (24‰ ; Figure 6). However, there still remains substantial variability at the level of individual homologues that appears to mask any relationship to environmental parameters. Further averaging the $\delta\text{D}_{\text{wax}}$ values of homologues reveals significant correlations with environmental parameters, albeit, to a lesser degree than that found in lake sediments.

These results indicate that it is possible to reconstruct δD_r based on soil $\delta\text{D}_{\text{wax}}$. Using the average soil $\delta\text{D}_{\text{wax}}$ can enable reconstructing δD_r to within $\pm 7\text{‰}$ (the standard deviation of the residuals of the correlation in Figure 5b) or an $\text{avg}\epsilon_{\text{app}} = -126 \pm 7\text{‰}$ (based on the average and 1σ of the ϵ_{app} , Table S2-3). As ϵ_{app} is affected by RH, independent knowledge of RH can help reduce the uncertainty in δD_r reconstructions. Alternatively, if δD_r is known independently, it could be possible (within the uncertainty) to reconstruct RH.

Leaf wax *n*-alkanes, which form in plants, get integrated into soils and are transported into lakes and oceans. By the time they are deposited in lakes, their $\delta\text{D}_{\text{wax}}$ (i.e., $\text{avg}\epsilon_{\text{app}}$) and $\delta^{13}\text{C}_{\text{wax}}$ variability is reduced substantially. Our results show that a significant portion of the homogenization process and variability reduction occurs during the initial incorporation of *n*-alkanes into soils and that even in young soils, the variability is reduced to an extent that significant correlations with environmental parameters can be observed.

7. Conclusion

The results of our field-based test of $\delta\text{D}_{\text{wax}}$, $\delta^{13}\text{C}_{\text{wax}}$, and chain length distributions of plants and soils along an $\sim 1,200\text{-mm/year}$ rainfall and $\sim 20\%$ relative humidity gradients in Israel provide empirical and quantitative information about the environmental and ecological parameters that control these parameters. In addition, we were able to quantifying the uncertainty of $\delta\text{D}_{\text{wax}}$ and $\delta^{13}\text{C}_{\text{wax}}$ in soils and their applicability to paleoclimate research. Our results show the following:

1. Soil $\delta^{13}\text{C}_{\text{wax}}$ in C_3 ecosystems is constant ($0.4\text{‰ } 1\sigma$) along an 800-mm/year rainfall gradient and is thus insensitive to rainfall amount, in contrast to published studies of plant leaf $\delta^{13}\text{C}$ values. Our data suggest $\delta^{13}\text{C}_{\text{wax}}$ may provide better quantification of landscape C_3/C_4 plant ratios than bulk $\delta^{13}\text{C}$.
2. Soil $\delta\text{D}_{\text{wax}}$ shows significant correlations with the isotopic composition of precipitation (δD_r), annual rainfall amount, and relative humidity of the growing season. The offset between δD_r and soil $\delta\text{D}_{\text{wax}}$ (ϵ_{app}) is significantly correlated with relative humidity. Thus, knowledge of past RH can reduce the uncertainty in δD_r reconstructions.
3. Plants that grow during the rainy season have ϵ_{app} that are $<10\text{‰}$ more depleted than plants that grow after the rainy season; however, this difference is not statistically significant, and therefore, in our data, seasonality does not contribute meaningfully to the total variability.
4. Soil $\delta\text{D}_{\text{wax}}$ and $\delta^{13}\text{C}_{\text{wax}}$ variability is reduced by $\sim 80\%$ compared to plant $\delta\text{D}_{\text{wax}}$ and $\delta^{13}\text{C}_{\text{wax}}$ variability.

Acknowledgments

We thank R. Boasson and S. Goldsmith for their help with fieldwork, the Lamont-Doherty Earth Observatory Organic Geochemistry group whose weekly discussions facilitated much of the ideas in this paper, and J. Nichols for help with figures. The field and analytical work was supported by an LDEO Climate Center grant (funded by the Vetlesen Foundation). Funding for instrumentation used in this study was provided by the Center for Climate and Life at Columbia University. We thank A. Diefendorf and an anonymous reviewer for their helpful comments on this manuscript and Sarah Feakins and two anonymous reviewers for constructive comments on a previous version of this manuscript. The full data set is provided in the supporting information. Lamont-Doherty Earth Observatory contribution number 8352.

References

- Aichner, B., Herzschuh, U., Wilkes, H., Vieth, A., & Böhner, J. (2010). δD values of *n*-alkanes in Tibetan lake sediments and aquatic macrophytes—A surface sediment study and application to a 16 ka record from Lake Koucha. *Organic Geochemistry*, *41*(8), 779–790. <https://doi.org/10.1016/j.orggeochem.2010.05.010>
- Ayalon, A., Bar-Matthews, M., & Schilman, B. (2004). Rainfall isotopic characteristics in various vites in Israel and the relationships with the unsaturated zone water. Geological survey of Israel Report, GSI/16/04. Jerusalem.
- Berke, M. A., Tipple, B. J., Hambach, B., & Ehleringer, J. R. (2015). Life form-specific gradients in compound-specific hydrogen isotope ratios of modern leaf waxes along a North American Monsoonal transect. *Oecologia*, *179*(4), 981–997. <https://doi.org/10.1007/s00442-015-3432-1>
- Bonnefille, R. (2010). Cenozoic vegetation, climate changes and hominid evolution in tropical Africa. *Global and Planetary Change*, *72*(4), 390–411. <https://doi.org/10.1016/j.gloplacha.2010.01.015>
- Burgoyne, T. W., & Hayes, J. M. (1998). Quantitative production of H_2 by pyrolysis of gas chromatographic effluents. *Analytical Chemistry*, *70*(24), 5136–5141. <https://doi.org/10.1021/ac980248v>
- Bush, R. T., & McInerney, F. A. (2013). Leaf wax *n*-alkane distributions in and across modern plants: Implications for paleoecology and chemotaxonomy. *Geochimica et Cosmochimica Acta*, *117*, 161–179. <https://doi.org/10.1016/j.gca.2013.04.016>
- Bush, R. T., & McInerney, F. A. (2015). Influence of temperature and C_4 abundance on *n*-alkane chain length distributions across the central USA. *Organic Geochemistry*, *79*, 65–73. <https://doi.org/10.1016/j.orggeochem.2014.12.003>
- Chikaraishi, Y., & Naraoka, H. (2006). Carbon and hydrogen isotope variation of plant biomarkers in a plant-soil system. *Chemical Geology*, *231*(3), 190–202. <https://doi.org/10.1016/j.chemgeo.2006.01.026>
- Chikaraishi, Y., Naraoka, H., & Poulson, S. R. (2004). Hydrogen and carbon isotopic fractionations of lipid biosynthesis among terrestrial (C_3 , C_4 and CAM) and aquatic plants. *Phytochemistry*, *65*(10), 1369–1381. <https://doi.org/10.1016/j.phytochem.2004.03.036>
- Collins, J. A., Schefuß, E., Mulitza, S., Prange, M., Werner, M., Tharammal, T., et al. (2013). Estimating the hydrogen isotopic composition of past precipitation using leaf-waxes from western Africa. *Quaternary Science Reviews*, *65*, 88–101. <https://doi.org/10.1016/j.quascirev.2013.01.007>
- Collister, J. W., Rieley, G., Stern, B., Eglinton, G., & Fry, B. (1994). Compound-specific $\delta^{13}C$ analyses of leaf lipids from plants with differing carbon dioxide metabolisms. *Organic Geochemistry*, *21*(6-7), 619–627. [https://doi.org/10.1016/0146-6380\(94\)90008-6](https://doi.org/10.1016/0146-6380(94)90008-6)
- d'Alpoim Guedes, J. A., Crabtree, S. A., Bocinsky, R. K., & Kohler, T. A. (2016). Twenty-first century approaches to ancient problems: Climate and society. *Proceedings of the National Academy of Sciences USA*, *113*(51), 14,483–14,491. <https://doi.org/10.1073/pnas.1616188113>
- deMenocal, P. B. (2011). Climate and human evolution. *Science*, *331*(6017), 540–542. <https://doi.org/10.1126/science.1190683>
- Diefendorf, A. F., Freeman, K. H., Wing, S. L., & Graham, H. V. (2011). Production of *n*-alkyl lipids in living plants and implications for the geologic past. *Geochimica et Cosmochimica Acta*, *75*(23), 7472–7485. <https://doi.org/10.1016/j.gca.2011.09.028>
- Diefendorf, A. F., & Freimuth, E. J. (2017). Extracting the most from terrestrial plant-derived *n*-alkyl lipids and their carbon isotopes from the sedimentary record: A review. *Organic Geochemistry*, *103*, 1–21. <https://doi.org/10.1016/j.orggeochem.2016.10.016>
- Diefendorf, A. F., Mueller, K. E., Wing, S. L., Koch, P. L., & Freeman, K. H. (2010). Global patterns in leaf ^{13}C discrimination and implications for studies of past and future climate. *Proceedings of the National Academy of Sciences*, *107*(13), 5738–5743. <https://doi.org/10.1073/pnas.0910513107>
- Farquhar, G., O'Leary, M., & Berry, J. (1982). On the relationship between carbon isotope discrimination and the intercellular carbon dioxide concentration in leaves. *Australian Journal of Plant Physiology*, *9*(2), 121. <https://doi.org/10.1071/PP9820121>
- Farquhar, G. D., Ehleringer, J. R., & Hubick, K. T. (1989). Carbon isotope discrimination and photosynthesis. *Annual Review of Plant Physiology and Plant Molecular Biology*, *40*(1), 503–537. <https://doi.org/10.1146/annurev.pp.40.060189.002443>
- Feakins, S. J., & Sessions, A. L. (2010). Controls on the D/H ratios of plant leaf waxes in an arid ecosystem. *Geochimica et Cosmochimica Acta*, *74*(7), 2128–2141. <https://doi.org/10.1016/j.gca.2010.01.016>
- Feakins, S. J., Wu, M. S., Ponton, C., Galy, V., & West, A. J. (2018). Dual isotope evidence for sedimentary integration of plant wax biomarkers across an Andes-Amazon elevation transect. *Geochimica et Cosmochimica Acta*, *242*, 64–81. <https://doi.org/10.1016/j.gca.2018.09.007>
- Ficken, K. J., Street-Perrott, F. A., Perrott, R. A., Swain, D. L., Olago, D. O., & Eglinton, G. (1998). Glacial/interglacial variations in carbon cycling revealed by molecular and isotope stratigraphy of Lake Nkunga, Mt. Kenya, East Africa. *Organic Geochemistry*, *29*(5-7), 1701–1719. [https://doi.org/10.1016/S0146-6380\(98\)00109-0](https://doi.org/10.1016/S0146-6380(98)00109-0)
- Freimuth, E. J., Diefendorf, A. F., & Lowell, T. V. (2017). Hydrogen isotopes of *n*-alkanes and *n*-alkanoic acids as tracers of precipitation in a temperate forest and implications for paleorecords. *Geochimica et Cosmochimica Acta*, *206*, 166–183. <https://doi.org/10.1016/j.gca.2017.02.027>
- Garcin, Y., Schefuß, E., Schwab, V. F., Garreta, V., Gleixner, G., Vincens, A., et al. (2014). Reconstructing C_3 and C_4 vegetation cover using *n*-alkane carbon isotope ratios in recent lake sediments from Cameroon, Western Central Africa. *Geochimica et Cosmochimica Acta*, *142*, 482–500. <https://doi.org/10.1016/j.gca.2014.07.004>
- Garcin, Y., Schwab, V. F., Gleixner, G., Kahmen, A., Todou, G., Séné, O., et al. (2012). Hydrogen isotope ratios of lacustrine sedimentary *n*-alkanes as proxies of tropical African hydrology: Insights from a calibration transect across Cameroon. *Geochimica et Cosmochimica Acta*, *79*, 106–126. <https://doi.org/10.1016/j.gca.2011.11.039>
- Goldsmith, Y., Polissar, P. J., Ayalon, A., Bar-Matthews, M., DeMenocal, P. B., & Broecker, W. S. (2017). The modern and Last Glacial Maximum hydrological cycles of the Eastern Mediterranean and the Levant from a water isotope perspective. *Earth and Planetary Science Letters*, *457*, 302–312. <https://doi.org/10.1016/j.epsl.2016.10.017>
- Graham, H. V., Patzkowsky, M. E., Wing, S. L., Parker, G. G., Fogel, M. L., & Freeman, K. H. (2014). Isotopic characteristics of canopies in simulated leaf assemblages. *Geochimica et Cosmochimica Acta*, *144*, 82–95. <https://doi.org/10.1016/j.gca.2014.08.032>
- Guenther, F., Aichner, B., Siegwolf, R., Xu, B., Yao, T., & Gleixner, G. (2013). A synthesis of hydrogen isotope variability and its hydrological significance at the Qinghai-Tibetan Plateau. *Quaternary International*, *313-314*, 3–16. <https://doi.org/10.1016/j.quaint.2013.07.013>
- Hartman, G., & Danin, A. (2010). Isotopic values of plants in relation to water availability in the Eastern Mediterranean region. *Oecologia*, *162*(4), 837–852. <https://doi.org/10.1007/s00442-009-1514-7>
- Hou, J., D'Andrea, W. J., & Huang, Y. (2008). Can sedimentary leaf waxes record D/H ratios of continental precipitation? Field, model, and experimental assessments. *Geochimica et Cosmochimica Acta*, *72*(14), 3503–3517. <https://doi.org/10.1016/j.gca.2008.04.030>

- Hou, J., D'Andrea, W. J., MacDonald, D., & Huang, Y. (2007). Hydrogen isotopic variability in leaf waxes among terrestrial and aquatic plants around Blood Pond, Massachusetts (USA). *Organic Geochemistry*, *38*(6), 977–984. <https://doi.org/10.1016/j.orggeochem.2006.12.009>
- Howard, S., McInerney, F. A., Caddy-Retalic, S., Hall, P. A., & Andrae, J. W. (2018). Modelling leaf wax *n*-alkane inputs to soils along a latitudinal transect across Australia. *Organic Geochemistry*, *121*, 126–137. <https://doi.org/10.1016/j.orggeochem.2018.03.013>
- Huang, Y., Eglinton, G., Ineson, P., Latter, P. M., Bol, R., & Harkness, D. D. (1997). Absence of carbon isotope fractionation of individual *n*-alkanes in a 23-year field decomposition experiment with *Calluna vulgaris*. *Organic Geochemistry*, *26*(7–8), 497–501. [https://doi.org/10.1016/S0146-6380\(97\)00027-2](https://doi.org/10.1016/S0146-6380(97)00027-2)
- Jia, G., Wei, K., Chen, F., & Peng, P. (2008). Soil *n*-alkane δD vs. altitude gradients along Mount Gongga, China. *Geochimica et Cosmochimica Acta*, *72*(21), 5165–5174. <https://doi.org/10.1016/j.gca.2008.08.004>
- Kahmen, A., Hoffmann, B., Schefuß, E., Arndt, S. K., Cernusak, L. A., West, J. B., & Sachse, D. (2013). Leaf water deuterium enrichment shapes leaf wax *n*-alkane δD values of angiosperm plants. II: Observational evidence and global implications. *Geochimica et Cosmochimica Acta*, *111*, 50–63. <https://doi.org/10.1016/j.gca.2012.09.004>
- Keeling, R. F., Piper, S. C., Bollenbacher, A. F., & Walker, S. J. (2010). Monthly atmospheric $^{13}C/^{12}C$ isotopic ratios for 11 SIO stations. In *Trends: A compendium of data on global change*. Oak Ridge, Tenn., U.S.A: Oak Ridge National Laboratory, U.S. Department of Energy.
- Kohn, M. J. (2016). Carbon isotope discrimination in C_3 land plants is independent of natural variations in pCO_2 . *Geochemical Perspectives Letters*, *2*, 35–43. <https://doi.org/10.7185/geochemlet.1604>
- Kohn, M. J. (2010). Carbon isotope compositions of terrestrial C_3 plants as indicators of (paleo)ecology and (paleo)climate. *Proceedings of the National Academy of Sciences of the United States of America*, *107*(46), 19,691–19,695. <https://doi.org/10.1073/pnas.1004933107>
- Levin, N. E. (2015). Environment and climate of early human evolution. *Annual Review of Earth and Planetary Sciences*, *43*(1), 405–429. <https://doi.org/10.1146/annurev-earth-060614-105310>
- Lichtfouse, É., Elbisser, B., Balesdent, J., Mariotti, A., & Bardoux, G. (1994). Isotope and molecular evidence for direct input of maize leaf wax *n*-alkanes into crop soils. *Organic Geochemistry*, *22*(2), 349–351. [https://doi.org/10.1016/0146-6380\(94\)90181-3](https://doi.org/10.1016/0146-6380(94)90181-3)
- Lichtfouse, É., Bardoux, G., Mariotti, A., Balesdent, J., Ballentine, D. C., & Macko, S. A. (1997). Molecular, ^{13}C , and ^{14}C evidence for the allochthonous and ancient origin of C_{16} - C_{18} *n*-alkanes in modern soils. *Geochimica et Cosmochimica Acta*, *61*(9), 1891–1898. [https://doi.org/10.1016/S0016-7037\(97\)00021-5](https://doi.org/10.1016/S0016-7037(97)00021-5)
- Lichtfouse, É., Chenu, C., Baudin, F., Leblond, C., Da Silva, M., Behar, F., et al. (1998). A novel pathway of soil organic matter formation by selective preservation of resistant straight-chain biopolymers: Chemical and isotope evidence. *Organic Geochemistry*, *28*(6), 411–415. [https://doi.org/10.1016/S0146-6380\(98\)00005-9](https://doi.org/10.1016/S0146-6380(98)00005-9)
- Magill, C. R., Ashley, G. M., Domínguez-Rodrigo, M., & Freeman, K. H. (2016). Dietary options and behavior suggested by plant biomarker evidence in an early human habitat. *Proceedings of the National Academy of Sciences*, *113*(11), 2874–2879. <https://doi.org/10.1073/pnas.1507055113>
- Magill, C. R., Ashley, G. M., & Freeman, K. H. (2013). Water, plants, and early human habitats in eastern Africa. *Proceedings of the National Academy of Sciences of the United States of America*, *110*(4), 1175–1180. <https://doi.org/10.1073/pnas.1209405109>
- Mazeas, L., Budzinski, H., & Raymond, N. (2002). Absence of stable carbon isotope fractionation of saturated and polycyclic aromatic hydrocarbons during aerobic bacterial biodegradation. *Organic Geochemistry*, *33*(11), 1259–1272. [https://doi.org/10.1016/S0146-6380\(02\)00136-5](https://doi.org/10.1016/S0146-6380(02)00136-5)
- Mendez-Millan, M., Nguyen Tu, T. T., Balesdent, J., Derenne, S., Derrien, D., Egasse, C., et al. (2014). Compound-specific ^{13}C and ^{14}C measurements improve the understanding of soil organic matter dynamics. *Biogeochemistry*, *118*(1–3), 205–223. <https://doi.org/10.1007/s10533-013-9920-7>
- National Research Council (2010). *Understanding climate's influence on human evolution*. *Human Evolution*. Washington D.C: The National Academies Press.
- Nguyen Tu, T. T., Derenne, S., Largeau, C., Bardoux, G., & Mariotti, A. (2004). Diagenesis effects on specific carbon isotope composition of plant *n*-alkanes. *Organic Geochemistry*, *35*(3), 317–329. <https://doi.org/10.1016/j.orggeochem.2003.10.012>
- Nguyen Tu, T. T., Egasse, C., Zeller, B., Bardoux, G., Biron, P., Ponge, J. F., et al. (2011). Early degradation of plant alkanes in soils: A litterbag experiment using ^{13}C -labelled leaves. *Soil Biology and Biochemistry*, *43*(11), 2222–2228. <https://doi.org/10.1016/j.soilbio.2011.07.009>
- O'Leary (1981). Carbon isotope fractionation in plants. *Phytochemistry*, *20*(4), 553–567. [https://doi.org/10.1016/0031-9422\(81\)85134-5](https://doi.org/10.1016/0031-9422(81)85134-5)
- Patalano, R., Wang, Z., Leng, Q., Liu, W., Zheng, Y., Sun, G., & Yang, H. (2015). Hydrological changes facilitated early rice farming in the lower Yangtze River Valley in China: A molecular isotope analysis. *Geology*, *43*(7), 639–642. <https://doi.org/10.1130/G36783.1>
- Pedentchouk, N., Freeman, K. H., & Harris, N. B. (2006). Different response of dD values of *n*-alkanes, isoprenoids, and kerogen during thermal maturation. *Geochimica et Cosmochimica Acta*, *70*(8), 2063–2072. <https://doi.org/10.1016/j.gca.2006.01.013>
- Peisker, M., & Henderson, S. A. (1992). Carbon: Terrestrial C_4 plants. *Plant, Cell & Environment*, *15*(9), 987–1004. <https://doi.org/10.1111/j.1365-3040.1992.tb01651.x>
- Peterse, F., van der Meer, M. T. J., Schouten, S., Jia, G., Ossebaar, J., Blokker, J., & Sinninghe Damsté, J. S. (2009). Assessment of soil *n*-alkane δd and branched tetraether membrane lipid distributions as tools for paleoelevation reconstruction. *Biogeosciences*, *6*(12), 2799–2807. <https://doi.org/10.5194/bg-6-2799-2009>
- Polissar, P. J., & D'Andrea, W. (2014). Uncertainty in paleohydrologic reconstructions from molecular δD values. *Geochimica et Cosmochimica Acta*, *129*, 146–156. <https://doi.org/10.1016/j.gca.2013.12.021>
- Polissar, P. J., & Freeman, K. H. (2010). Effects of aridity and vegetation on plant-wax δD in modern lake sediments. *Geochimica et Cosmochimica Acta*, *74*(20), 5785–5797. <https://doi.org/10.1016/j.gca.2010.06.018>
- Pond, K. L., Huang, Y., Wang, Y., & Kulpa, C. F. (2002). Hydrogen isotopic composition of individual *n*-alkanes as an intrinsic tracer for bioremediation and source identification of petroleum contamination. *Environmental Science and Technology*, *36*(4), 724–728. <https://doi.org/10.1021/es011140r>
- Potts, R. (1996). Evolution and climate variability. *Science*, *273*(5277), 922–923. <https://doi.org/10.1126/science.273.5277.922>
- Quade, J. (2014). The Carbon, Oxygen, and Clumped Isotopic Composition of Soil Carbonate in Archeology. *Treatise on Geochemistry*. In (2nd ed., Vol. 14). Elsevier Ltd. <https://doi.org/10.1016/B978-0-08-095975-7.01211-0>
- Rommerskirchen, F., Plader, A., Eglinton, G., Chikaraishi, Y., & Rullkötter, J. (2006). Chemotaxonomic significance of distribution and stable carbon isotopic composition of long-chain alkanes and alkan-1-ols in C_4 grass waxes. *Organic Geochemistry*, *37*(10), 1303–1332. <https://doi.org/10.1016/j.orggeochem.2005.12.013>

- Sachse, D., Billault, I., Bowen, G. J., Chikaraishi, Y., Dawson, T. E., Feakins, S. J., et al. (2012). Molecular paleohydrology: Interpreting the hydrogen-isotopic composition of lipid biomarkers from photosynthesizing organisms. *Annual Review of Earth and Planetary Sciences*, 40(1), 221–249. <https://doi.org/10.1146/annurev-earth-042711-105535>
- Sachse, D., Radke, J., & Gleixner, G. (2004). Hydrogen isotope ratios of recent lacustrine sedimentary *n*-alkanes record modern climate variability. *Geochimica et Cosmochimica Acta*, 68(23), 4877–4889. <https://doi.org/10.1016/j.gca.2004.06.004>
- Sachse, D., Radke, J., & Gleixner, G. (2006). δD values of individual *n*-alkanes from terrestrial plants along a climatic gradient—Implications for the sedimentary biomarker record. *Organic Geochemistry*, 37(4), 469–483. <https://doi.org/10.1016/j.orggeochem.2005.12.003>
- Schefuß, E., Ratmeyer, V., Stuut, J.-B. W., Jansen, J. H. F., & Sinninghe Damsté, J. S. (2003). Carbon isotope analyses of *n*-alkanes in dust from the lower atmosphere over the central eastern Atlantic. *Geochimica et Cosmochimica Acta*, 67(10), 1757–1767. [https://doi.org/10.1016/S0016-7037\(02\)01414-X](https://doi.org/10.1016/S0016-7037(02)01414-X)
- Schubert, B. A., & Jahren, A. H. (2012). The effect of atmospheric CO₂ concentration on carbon isotope fractionation in C₃ land plants. *Geochimica et Cosmochimica Acta*, 96, 29–43. <https://doi.org/10.1016/j.gca.2012.08.003>
- Schwab, V. F., Garcin, Y., Sachse, D., Todou, G., Séné, O., Onana, J.-M., et al. (2015). Effect of aridity on $\delta^{13}C$ and δD values of C₃ plant- and C₄ graminoid-derived leaf wax lipids from soils along an environmental gradient in Cameroon (Western Central Africa). *Organic Geochemistry*, 78, 99–109. <https://doi.org/10.1016/j.orggeochem.2014.09.007>
- Shelach-Lavi, G., Teng, M., Goldsmith, Y., Wachtel, I., Stevens, C. J., Marder, O., et al. (2019). Sedentism and plant cultivation in northeast China emerged during affluent conditions. *PLoS ONE*, 14(7) e0218751. <https://doi.org/10.1371/journal.pone.0218751>
- Sessions, A. L., Burgoyne, T. W., & Hayes, J. M. (2001). Correction of H₃⁺ contributions in hydrogen isotope ratio monitoring mass spectrometry. *Analytical Chemistry*, 73(2), 192–199. <https://doi.org/10.1021/ac000489e>
- Smith, F. A., & Freeman, K. H. (2006). Influence of physiology and climate on δD of leaf wax *n*-alkanes from C₃ and C₄ grasses. *Geochimica et Cosmochimica Acta*, 70(5), 1172–1187. <https://doi.org/10.1016/j.gca.2005.11.006>
- Soil Survey Staff (1999). Soil taxonomy. *Soil Taxonomy A Basic System of Soil Classification for Making and Interpreting Soil Surveys*, 114(6), 492–493. <https://doi.org/10.1017/S0016756800045489>
- Tipple, B. J., Berke, M. A., Doman, C. E., Khachatryan, S., & Ehleringer, J. R. (2013). Leaf-wax *n*-alkanes record the plant-water environment at leaf flush. *Proceedings of the National Academy of Sciences*, 110(7), 2659–2664. <https://doi.org/10.1073/pnas.1213875110>
- Tipple, B. J., Berke, M. A., Hambach, B., Roden, J. S., & Ehleringer, J. R. (2014). Predicting leaf wax *n*-alkane ²H/¹H ratios: Controlled water source and humidity experiments with hydroponically grown trees confirm predictions of Craig-Gordon model. *Plant, Cell & Environment*, 38(6), 1035–1047. <https://doi.org/10.1111/pce.12457>
- Tipple, B. J., & Pagani, M. (2010). A 35Myr North American leaf-wax compound-specific carbon and hydrogen isotope record: Implications for C₄ grasslands and hydrologic cycle dynamics. *Earth and Planetary Science Letters*, 299(1–2), 250–262. <https://doi.org/10.1016/j.epsl.2010.09.006>
- Tipple, B. J., & Pagani, M. (2013). Environmental control on eastern broadleaf forest species' leaf wax distributions and d/h ratios. *Geochimica et Cosmochimica Acta*, 111, 64–77. <https://doi.org/10.1016/j.gca.2012.10.042>
- Tuthorn, M., Zech, R., Ruppenthal, M., Oelmann, Y., Kahmen, A., del Valle, H. F., et al. (2015). Coupling d²H and d¹⁸O biomarker results yields information on relative humidity and isotopic composition of precipitation—A climate transect validation study. *Biogeosciences*, 12(12), 3913–3924. <https://doi.org/10.5194/bg-12-3913-2015>
- Uno, K. T., Polissar, P. J., Kahle, E., Feibel, C., Harmand, S., Roche, H., & DeMenocal, P. B. (2016). A Pleistocene palaeovegetation record from plant wax biomarkers from the Nachukui Formation, West Turkana, Kenya. *Philosophical Transactions of the Royal Society, B: Biological Sciences*, 371(1698). <https://doi.org/10.1098/rstb.2015.0235>
- Vogel, J. C., Fuls, A., & Danin, A. (1986). Geographical and environmental distribution of C₃ and C₄ grasses in the Sinai, Negev, and Judean deserts. *Oecologia*, 70(2), 258–265. <https://doi.org/10.1007/BF00379249>
- Vogts, A., Schefuß, E., Badewien, T., & Rullkötter, J. (2012). *n*-Alkane parameters from a deep sea sediment transect off southwest Africa reflect continental vegetation and climate conditions. *Organic Geochemistry*, 47, 109–119. <https://doi.org/10.1016/j.orggeochem.2012.03.011>
- Wei, K., & Jia, G. (2009). Soil *n*-alkane $\delta^{13}C$ along a mountain slope as an integrator of altitude effect on plant species $\delta^{13}C$. *Geophysical Research Letters*, 36, L11401. <https://doi.org/10.1029/2009GL038294>
- Wiesenberg, G. L. B., Schwarzbauer, J., Schmidt, M. W. I., & Schwark, L. (2004). Source and turnover of organic matter in agricultural soils derived from *n*-alkane/*n*-carboxylic acid compositions and C-isotope signatures. *Organic Geochemistry*, 35(11–12), 1371–1393. <https://doi.org/10.1016/j.orggeochem.2004.03.009>
- Winter, K., & Troughton, J. H. (1978). Photosynthetic pathways in plants of coastal and inland habitats of Israel and the Sinai. *Flora*, 167(1), 1–34. [https://doi.org/10.1016/S0367-2530\(17\)31087-3](https://doi.org/10.1016/S0367-2530(17)31087-3)
- Wu, M. S., Feakins, S. J., Martin, R. E., Shenkin, A., Bentley, L. P., Blonder, B., et al. (2017). Altitude effect on leaf wax carbon isotopic composition in humid tropical forests. *Geochimica et Cosmochimica Acta*, 206, 1–17. <https://doi.org/10.1016/j.gca.2017.02.022>
- Zech, M., Pedentchouk, N., Buggle, B., Leiber, K., Kalbitz, K., Marković, S. B., & Glaser, B. (2011). Effect of leaf litter degradation and seasonality on D/H isotope ratios of *n*-alkane biomarkers. *Geochimica et Cosmochimica Acta*, 75(17), 4917–4928. <https://doi.org/10.1016/j.gca.2011.06.006>
- Ziv, B., Dayan, U., Kushnir, Y., Roth, C., & Enzel, Y. (2006). Regional and global atmospheric patterns governing rainfall in the southern Levant. *International Journal of Climatology*, 26(1), 55–73. <https://doi.org/10.1002/joc.1238>
- Zomer, R. J., Trabucco, A., Bossio, D. A., & Verchot, L. V. (2008). Climate change mitigation: A spatial analysis of global land suitability for clean development mechanism afforestation and reforestation. *Agriculture, Ecosystems and Environment*, 126(1–2), 67–80. <https://doi.org/10.1016/j.agee.2008.01.014>